Optimal energy management in all-electric residential energy systems with heat and electricity storage

Tom Terlouw[a,b,*], Tarek AlSkaif[a], Christian Bauer[b], Wilfried van Sark[a]

[a] *Copernicus Institute of Sustainable Development, Utrecht University, Princetonlaan 8a, 3584 CB Utrecht, the Netherlands*
[b] *Paul Scherrer Institute, Laboratory for Energy Systems Analysis, 5232, Villigen PSI, Switzerland*

HIGHLIGHTS

- Optimization of HES and CES with heat and electricity storage.
- An optimization model is developed and is tested on a community in Switzerland.
- CES performs better than HES on both economic and environmental performance.
- HES and CES are currently non-profitable.
- Economic feasibility can be obtained with a larger heat storage medium.

ARTICLE INFO

ABSTRACT

Residential demand profiles typically demonstrate a mismatch between energy demand and PV supply. Different solutions are proposed, such as demand side management and energy storage systems. Nevertheless, costs and environmental impacts of some technologies (e.g. batteries) are high. This paper proposes two system designs: Home Energy Storage (HES) and Community Energy Storage (CES). Besides electricity storage, heat storage is used in the two system designs to supply domestic hot water and space heating. Furthermore, the trade-offs between the different storage mediums in relation to costs are analyzed. To achieve that, different methodologies are used to size the electricity and heat storage mediums for HES and CES. Next, a multi-objective mixed integer linear programming model is developed to optimize the operation costs and CO_2-emissions for each system design. After that, the model is tested on a residential community situated in Cernier (Switzerland). The results demonstrate that CES performs better than HES on economic and environmental performance due to economies of scale and the optimally sized storage capacity of the battery in CES. Currently, none of the proposed system designs is economically feasible. However, the sensitivity analysis shows that a profitable system design can be obtained for both HES and CES, when the electricity storage (i.e. battery storage) size is reduced and the heat storage (i.e. water storage tank) size is increased.

1. Introduction

The built environment is the largest energy consuming sector and accounts for more than one third of global energy demand [1,2]. Consequently, policy and regulations embrace beneficial incentives to reduce residential energy demand and CO_2-emissions by stimulating renewable distributed energy resources [2]. At the moment, electricity generation from solar Photovoltaic (PV) is the fastest growing distrubuted energy resource and could reach 22% of global electricity generation in 2050 [3].

In Europe, the most applied incentive schemes to stimulate solar PV generation on residential rooftops are feed-in tariffs [4]. Feed-in tariffs provide reimbursement to residential households for the generation of rooftop PV electricity. Households typically receive a subsidy when electricity is fed back into the grid [5]. Current developments reveal that an increasing amount of countries will decrease their feed-in tariff compensation in the near future, since grid parity and policy goals are reached (e.g. as in Germany [6] and Switzerland [7]). Therefore, alternative strategies are implemented to obtain a profitable operation from distributed energy resources. One of the fastest growing

Nomenclature

Abbreviations

ASHP	Air-to-water Source Heat Pump
DHW	Domestic Hot Water
BEV	Battery Electric Vehicle
CES	Community Energy Storage
CES_{opt}	CES alternative with optimally sized battery
CoP	Coefficient of Performance
DSM	Demand Side Management
EMS	Energy Management System
HES	Home Energy Storage
HES_{opt}	HES alternative with optimally sized battery
HES_{std}	HES alternative with standardized battery size
LCA	Life Cycle Assessment
LCOE	Levelized Costs Of Electricity
NMC	Nickel-Manganese-Cobalt oxide
PBP	Pay-Back-Period
PV	Photovoltaic
PVSC	PV-Self-Consumption
SH	Space Heating
SoC	State of Charge
WST	Water Storage Tank
WST_{DHW}	Water Storage Tank (Domestic Hot Water part)
WST_{SH}	Water Storage Tank (Space Heating part)

Indices

a	index for shiftable load, $a \in \{1, 2, ..., A\}$
i	index for households, $i \in \{1, 2, ..., N\}$
t	index for time-slots, $t \in \{1, 2, ..., T\}$

Sets

$\mathcal{A}$	set of shiftable devices
$\mathcal{N}$	set of households
$\mathcal{T}$	set of time-slots

Parameters

ρ_{water}	water density [kg l^{-1}]
η_{ch}	battery charging efficiency [–]
η_{dis}	battery discharging efficiency [–]
a_0, a_1, a_2	model coefficients for ASHP or for specific heating distribution system [–]
A_{tank}	total surface area of the WST [m^2]
c	specific heat capacity of water [kW h kg^{-1}K^{-1}]
c^t	cost of grid power absorbed at t [euro/kW h]
c^t_{we}	wholesale electricity price at t [euro/kW h]
C^i_{bat}	optimally battery storage capacity in i [kW h]
$C^i_{bat,CES}$	battery storage size in CES in i [kW h]
C_l	capacity start for economies of scale [kW h]
C_{nom}	nominal installed capacity [kW h]
$C^i_{DHW,tank}$	mass of storage for DHW in i [kg]
$C^i_{SH,tank}$	mass of storage for SH in i [kg]
$Cap_{CES,opt}$	total optimum capacity of battery in CES [kW h]
CoP	mean CoP based on SH and DHW mode [–]
CoP^t_{DHW}	CoP for DHW mode at t [–]
CoP^t_{SH}	CoP for SH mode at t [–]
CoP_{min}	minimum expected CoP [–]
$Cost_{ASHP,CES}$	cost of the ASHP in CES [euro]
$Cost_{sm}$	cost of the storage medium [euro]
$cost_{rel}$	relative cost of the technology [euro/kW h]
$D^{t,i}_{DHW}$	heat demand based on the heat demand profile for DHW at t in i [kW]
$D^{t,i}_{SH}$	heat demand based on the heat demand profile for SH at t in i [kW]
E^i_{inj}	maximum daily injected electricity to the grid the battery should be able to store in i [kW h]
E^a_{sl}	daily electricity consumption of a [kW h]
g^t	carbon intensity of grid power absorbed at t [kg CO$_2$ eq./kW h]
$n^i_{persons}$	number of persons in i [–]
$P^i_{bat,max}$	maximum power the battery can (dis-)charge in i [kW]
$P^i_{grid,max}$	maximum allowed power from/to the grid in i [kW]
$P^i_{hp,installed}$	installed power size of the heat pump in i [kW]
P^a_{max}	upper limit of power assignment to a [kW]
P^a_{min}	lower limit of power assignment to a [kW]
$P^{t,i}_{nsl}$	non-shiftable load at t in i [kW]
$P^{t,i}_{peak}$	maximum allowed power load at t in i [kW]
$P^{t,i}_{PV}$	amount of power obtained from PV system at t in i [kW]
$P^i_{ramprate,max}$	maximum ramp rate the heat pump can operate in i [kW]
Q^i_{peak}	maximum heat demand load in i [kW]
$Q^i_{storage,DHW}$	heat storage capacity for DHW in i [kW h]
$Q^i_{storage,SH}$	heat storage capacity for SH in i [kW h]
S_{DHW}	share of DHW of the WST based on volume [–]
S_{SH}	share of SH of the WST based on volume [–]
Sb^i	share of CES in i [–]
SoC_0	initial battery SoC [%]
SoC_{max}	maximum battery SoC [%]
SoC_{min}	minimum battery SoC [%]
ΔT	temperature difference between the outside environment and supply temperature [K]
T^t_{amb}	ambient temperature at t [K]
$T^i_{building,max}$	maximum inside building temperature in i [K]
$T^i_{building,min}$	minimum inside building temperature in i [K]
$T^i_{DHW,max}$	maximum water temperature of upper WST for DHW mode in i [K]
$T^i_{DHW,min}$	minimum water temperature of upper WST for DHW mode in i [K]
$T^i_{SH,max}$	maximum water temperature of lower WST for SH mode in i [K]
$T^i_{SH,min}$	minimum water temperature of lower WST for SH mode in i [K]
$T^t_{supply,min,SH}$	minimum supply water temperature of the WST for SH at t [K]
U^i	thermal heat loss of the building in i [kW K^{-1}]
$TP^{a,t,i}$	time preference for the activation of a at t in i [–]
U_{tank}	specific heat loss of the WST [kW m^{-2}K^{-1}]
V^i_{DHW}	volume of the WST for DHW in i [l]
V^i_{SH}	volume of the WST for SH in i [l]
$V_{SH,Qpeak}$	amount of volume of WST_{SH} based on peak heat demand [l kW^{-1}]

Variables

$k^{t,i}_{building}$	inside building temperature at t in i [K]
$p^{a,t,i}$	power demand of a at t in i [kW]
$p^{t,i}$	power demand at t in i [kW]
$p^{t,i}_{hp}$	electricity load of the heat pump at t in i [kW]
$p^{t,i}_{bat,ch}$	battery charging power at t in i [kW]
$p^{t,i}_{bat,dis}$	battery discharging power at t in i [kW]
$p^{t,i}_{dhw}$	electricity for DHW demand from the heat pump at t in i [kW]
$p^{t,i}_{grid,abs}$	power absorbed from the grid at t in i [kW]
$p^{t,i}_{grid,inj}$	power injected into the grid at t in i [kW]
$p^{t,i}_{sh}$	electricity for SH demand from the heat pump at t in i [kW]
$p^{t,i}_{sl}$	shiftable load at t in i [kW]

$q_{dhw}^{t,i}$	heat provided of the heat pump for DHW demand at t in i [kW]		$CO_{2avoided}^{i}$	CO$_2$-emissions of alternative during lifetime in i [kg CO$_2$-eq.]
$q_{hp}^{t,i}$	total heat provided of the heat pump at t in i [kW]			CO$_2$-emissions avoided during lifetime in i [kg CO$_2$-eq.]
$q_{sh}^{t,i}$	heat provided of the heat pump for SH demand at t in i [kW]		$CO_{2baseline}^{i}$	CO$_2$-emissions of baseline during lifetime in i [kg CO$_2$-eq.]
$SoC^{t,i}$	battery state of charge at t in i [%]		G	CO$_2$-intensity of electricity delivered during lifetime [kg CO$_2$-eq./kW h]
$u_{sh}^{t,i}$	flexible SH supply to compensate heat loss of the building at t in i [kW]		g_{annual}^{i}	annual CO$_2$-emissions from system operation in i [kg CO$_2$ eq./year]
$u_{tank}^{t,i}$	total heat loss from WST at t in i [kW]		I_{CES}	investment costs for CES [euro]
$u_{tank,dhw}^{t,i}$	heat loss of upper part of WST for DHW demand at t in i [kW]		I_{HES}	investment costs for HES [euro]
$u_{tank,sh}^{t,i}$	heat loss of lower part of WST for SH demand at t in i [kW]		L	lifetime of system [years]
$w_{dhw}^{t,i}$	water temperature of upper WST for DHW mode at t in i [K]		$LCOE^{i}$	levelized costs of electricity in i [euro/kW h]
			PBP_{CES}^{i}	number of years before recovering initial investment in CES in i [years]
$w_{sh}^{t,i}$	water temperature of lower WST for SH mode at t in i [K]		PBP_{HES}^{i}	number of years before recovering initial investment in HES i [years]
$y^{a,t,i}$	binary decision variable when a can be operated at t in i [–]		$PVSC^{i}$	PV-self-consumption ratio in i [–]
			R^{i}	cost reduction compared to reference scenario due to the reduction of energy absorbed from the power and gas grid in i [euro]
Economics			γ	interest rate [%]
c_{annual}^{i}	annual electricity costs for system operation in i [euro/year]			
$c_{maintenance}^{i}$	annual maintenance cost in i [euro/year]			

alternative strategies is maximizing the local consumption of self-generated PV electricity, also known as PV-Self-Consumption (PVSC) [8].

However, the supply of solar electricity is volatile due to the daily and seasonal fluctuations of solar irradiation. Residential demand profiles demonstrate peaks during evening and morning hours, while PV power peaks are usually generated around noon [9]. Consequently, the supply of solar electricity results in a mismatch with current demand profiles. This mismatch results in a low PVSC hence different solutions are proposed, such as Demand Side Management (DSM) and energy storage systems. DSM refers to "the actions that influence the way consumers use electricity in order to achieve savings and higher efficiency in energy use" [10]. Besides DSM, energy storage systems can be useful when the amount of intermittent energy sources is increased since it improves the dispatchability of renewable energy technologies [8].

Different types of energy storage systems can be implemented, such as electricity storage (e.g. batteries) and heat storage (e.g. Water Storage Tanks (WSTs)) [11,12]. At the moment, the most common form of residential energy storage is Home Energy Storage (HES), where the storage medium is situated within a residential household. However, recent research [13–17] demonstrates that Community Energy Storage (CES) can offer additional benefits, such as other power applications (e.g. peak shaving) and economies of scale [8,16,18,19]. Consequently, CES raises attention and is recently introduced as assessment scale in the built environment [8].

One of the developments related to HES and CES is the concept of all-electric smart microgrids in which distributed energy resources and localized energy storage systems are controlled by an Energy Management System (EMS), which can provide different applications (e.g. PVSC and DSM) [17]. In addition, the integration of shiftable loads (e.g. heat pumps and Battery Electric Vehicles (BEVs)) can offer flexibility to energy systems [20,21]. The concept of all-electric microgrids is lately introduced to substitute fossil-fuel based energy systems, due to more aggressive policy on climate change [22]. However, costs and environmental impacts of some technologies are still high (e.g. batteries) [23].

Consequently, it is essential to evaluate alternative energy systems on economic feasibility and environmental performance. Many studies and optimization models are proposed to evaluate costs of alternative energy systems for different storage scales (i.e. HES and CES). For example, the work of [19] proposed a multi-objective optimization model

to assess the economic and environmental potential of energy arbitrage in CES systems, from the perspective of an aggregator and a distribution system operator. However, the work of [19] excluded HES and neglected the economic and environmental potential of energy storage from the perspective of residential households. Furthermore, [17] proposed a CES system where households share the CES system by making use of an EMS, to manage the allocation of the available energy in the storage unit. The work of [24] examined additional benefits of CES systems and proposed a strategy to determine all potential benefits and costs of CES deployment to a utility for optimal allocation of multiple CES units in a distribution system with PV generation. Furthermore, [13] proposed an algorithm to determine additional benefits of CES by taking advantage of competitive energy markets. Besides, [16] compared HES and CES in the perspective of residential households. The authors of [16] created an optimization model to compare the technical and economic feasibility of HES with CES with different methodologies to size the batteries, based on a case study in the Netherlands. Their work is focused on battery energy storage and neglected the environmental performance of HES and CES and other storage technologies. The authors of [25] developed an optimization method for the optimal operation and design of multi-energy systems with seasonal energy storage and applied this framework on a Swiss case study. The work of [25] also included various storage technologies (such as batteries and hydrogen storage) and their environmental performance (i.e. CO$_2$-emissions). Furthermore, [26] assessed the techno-economic benefits of CES battery systems as a function of the size of the community to perform both demand load shifting and PV energy time-shift in the United Kingdom. Additionally, [27] proposed an optimization model and presented an economic analysis of a CES system while participating in different energy markets.

The above section demonstrates that detailed case studies which compare different storage scales (HES and CES), include various storage mediums (heat and electricity storage), include total residential energy demand (i.e. heating and electricity) and optimize both operation costs and CO$_2$-emissions from the perspective of the end-user customer over a longer assessment period, are missing in the literature. Also, the trade-offs between storage mediums (electricity and heat storage) in relation to costs and CO$_2$-emissions is still a research gap. Our work aims to close these research gaps. Therefore, the contribution of our paper can be summarized as follows:

- A comprehensive techno-economic and environmental assessment of different storage scales: HES and CES.
- To achieve this, an optimization model is formulated which optimizes both operation costs and CO_2-emissions with an assessment period of one year.
- The model includes different flexible demand loads (i.e. BEVs and heat pumps) of all-electric residential energy systems and covers the total energy demand of households.
- The optimization model combines different storage mediums (electricity and heat storage). In addition, the trade-offs between different type of storage mediums (electricity and heat storage) in relation to costs are analyzed in the sensitivity analysis.
- The optimization model is applied on a realistic case study in Switzerland.

To achieve this, different all-electric alternatives are assessed on their economic and environmental performance in the perspective of residential households, to substitute fossil-fuel based residential energy systems. We use mixed integer linear programming to optimize the energy systems, since earlier research demonstrates that this approach is an accurate and well-established methodology to optimize and compare the performance of different system designs [16,28]. In addition, this method has been widely used in the energy field [13,16,17,19,25].

Our paper enables other researchers to identify further improvements and drivers for the development of future residential energy systems, based on different storage scales (HES and CES). Furthermore, our research could help policy-makers and relevant stakeholders to support the most promising storage alternative (HES or CES) in the built environment during system operation or system lifetime. In addition, our work could encourage end-user customers to invest in a certain (sustainable) system design or technology.

The procedure of this paper is as follows: the technology description is provided in Section 2. Next, system specifications of HES and CES are formulated in Section 3. After that, the optimization problem is developed under a set of constraints in Section 4. Section 5 provides explanation of the economic and environmental performance indicators. After that, data collection for the case study is discussed in Section 6. In Section 7, the results are provided for different energy systems. Finally, the discussion and conclusion are given in Section 8 and 9, respectively.

2. Technology description

In this paper, a set of households $\mathcal{N}$ is considered, indexed by $i \in \{1, 2, ..., N\}$. Their heat and electricity supply is described by a load profile, where their demand and supply can be delivered by different system components during a timeslot, $t \in \mathcal{T} = \{t_0, t_0 + \Delta t, t_0 + 2\Delta t, ..., T\}$. The considered number of timeslots for a time horizon is represented by T. The load of devices can be divided into a shiftable and non-shiftable load profile to indicate the demand load shifting potential. Shiftable loads (e.g. washing machines) are devices that can be scheduled at another suitable time hence can be used for DSM purposes. While non-shiftable loads (e.g. TV) are bound to a fixed operational period hence cannot be used for DSM strategies [29]. A^i represents the number of shiftable devices in household *i*. The most important system components will be discussed in the following sections.

2.1. Energy management system

The home EMS controls the power flows and loads of the system. Additionally, different information control flows between technologies are exchanged for the controlling and scheduling of system components and devices. The EMS minimizes the amount of electricity absorbed from the electricity grid by optimizing the utilization of self-produced PV electricity. This is achieved by direct consumption of PV electricity,

by storing the surplus electricity in the battery, and/or by using it to heat water in the WST with a heat pump. This is performed by an optimization algorithm.

2.2. Air-to-water source heat pump

Different heat pumps can be used to deliver Space Heating (SH) and Domestic Hot Water (DHW) demand. However, we only consider Air-to-water Source Heat Pumps (ASHPs) for the following reasons. ASHPs can be easily installed in order to retrofit houses, they can provide both SH and DHW simultaneously, they have a small ground area requirement and are practical in populated urban areas [30], and therefore seem to be the preferred heating technology for the future. A simplified Coefficient of Performance (CoP) model of an ASHP fleet is used to predict the CoP at hourly resolution which serves as input for the optimization model. This CoP model is derived from [31].

To further increase accurateness, the predicted CoP is calculated separately for SH (CoP_{SH}^t) and DHW (CoP_{DHW}^t). Where a_0, a_1 and a_2 are model coefficients for an ASHP and are specified on 5.06, -0.05 and 0.00006, respectively [31]. The supply temperature of DHW is typically around 323 K, while the supply temperature of SH is lower and is around 313 K [30].

$$CoP_{\text{SH}}^t \ \& \ CoP_{\text{DHW}}^t = a_0 + a_1 \Delta T + a_2 \Delta T^2, \tag{1}$$

where ΔT is the temperature difference between the outside environment and the supply temperature [K].

A bivalent or monovalent ASHP can be used. The bivalent system has an electrical back-up heater for cold days. In this work, only monovalent heat pump systems are considered since this reduces the system complexity significantly. The ASHP is sized to supply the annual peak of the heat demand of household *i* (Q_{peak}^i) [32] divided by the minimum expected CoP (CoP_{min}) to provide sufficient heating during cold days. The following equation is used to determine the power size ($P_{\text{hp,installed}}^i$) of the ASHP.

$$P_{\text{hp,installed}}^i = \frac{Q_{\text{peak}}^i}{CoP_{\text{min}}}. \tag{2}$$

Hot water storage is required to deliver heat for DHW and SH demand. Therefore, a WST is installed due to its relatively low costs and easy implementation [11]. The ASHP consumes electricity to heat water by a heat exchanger. After that, the water flows to the WST where it can be stored for a certain time. We assume that the ASHP can operate in DHW mode and SH mode. This means that the ASHP can generate different water temperatures to the WST simultaneously. The WST composes of a DHW and SH layer. The DHW layer is the upper part of the WST (denoted as WST_{DHW}), since hot water typically accumulates to the upper part of the WST. Consequently, the lower part of the WST covers the SH layer (denoted as WST_{SH}). For WST_{SH}, the heat flows to the low temperature floor heating system where it supplies heat to the inside building environment. With this approach some assumptions must be made [33].

Firstly, the temperature of WST_{DHW} is higher than or equal to the temperature of WST_{SH} to build stratified water layers. Secondly, the ASHP can operate on PV, battery and grid electricity. Also, the stratified layers have negligible mixing since they are separated by a thermocline. In addition, water storage in the heating distribution system is not included.

Next, the sizes of the WST for both WST_{DHW} and WST_{SH} mode need to be specified. The following equations are proposed to determine the volume of WST_{DHW} (V_{DHW}^i), the volume of WST_{SH} (V_{SH}^i), heat storage of WST_{DHW} ($Q_{\text{storage,DHW}}^i$) and heat storage WST_{SH} ($Q_{\text{storage,SH}}^i$) and are derived from [32]. 1.25 represents a safety factor to store sufficient DHW.

$$V_{\text{DHW}}^i = 1.25 \cdot 65 \cdot n_{\text{persons}}^{i \ 0.7}, \tag{3}$$

where n_{persons}^i are the number of persons in *i* [–].

The total amount of heat storage capacity of WST$_{DHW}$ ($Q^i_{storage,DHW}$) partly depends on the minimum ($T^i_{DHW,min}$) and maximum ($T^i_{DHW,max}$) water temperature of WST$_{DHW}$. The heat storage capacity of WST$_{SH}$ ($Q^i_{storage,SH}$) can be calculated with the same methodology.

$$Q^i_{storage,DHW} = V^i_{DHW}\rho_{water}c(T^i_{DHW,max} - T^i_{DHW,min}),$$ (4)

where ρ_{water} is water density [kg l^{-1}] and c is the specific heat capacity of water [kW h kg^{-1} K^{-1}].

We decide to minimize the WST to avoid large area requirements within residential buildings. For WST$_{SH}$ mode, a minimum storage size of 10–20 l (per kW heat peak demand, denoted as $V_{SH,Qpeak}$) is recommended for heat pumps with variable speed [32]. Note that the considered heat pump is a monovalent heat pump hence there is no back up heater installed. Therefore, the upper amount ($V_{SH,Qpeak} = 20 l kW^{-1}$) of the minimum recommended WST$_{SH}$ storage size is installed.

$$V^i_{SH} = V_{SH,Qpeak} \cdot Q^i_{peak}.$$ (5)

For WST$_{SH}$, a heating distribution system is required. Every type of heating distribution system has its own "heating curve" where the minimum supply temperature ($T^t_{supply,min,SH}$) of the WST is given by Eq. (6), adopted from [31]. This equation is valid for outside temperatures (T^t_{amb}) lower than 15 °C. We adopt a low temperature heating system named as "A-10/W38" [31]. The distribution system coefficients for a_0, a_1 and a_2, are specified on 32.84, −0.56 and −0.0051, respectively [31]. Note that in this equation T^t_{amb} represents °C instead of Kelvin as unit for the temperature. 273 represents the conversion from °C into Kelvin.

$$T^t_{supply,min,SH} = 273 + a_0 + a_1 T^t_{amb} + a_2 T^{t\,2}_{amb}.$$ (6)

For DHW, we assume that the minimum supply temperature is independent on the outside temperature and is defined on the average of the maximum and minimum supply temperature of DHW.

2.3. Battery energy storage system

A battery is installed for electrical energy storage to increase the flexibility of the system. Since the model aims to minimize costs and CO$_2$-emissions by maximizing the PV generation, it follows that the amount of grid injection should be minimized. The daily injected electricity (E_{inj}) is obtained by using a histogram where the amount of daily grid injection is plotted, as described in [16]. This histogram is used to determine the storage size, where the battery should be able to store a certain percentage of the daily injected PV electricity.

However, there is also heat storage available in the WST (see Eq. (4)). Therefore, the required battery capacity, to store a certain percentage of grid electricity, is reduced by the already available heat storage capacity of the WST to avoid large and uneconomical sizing of the battery. The following equation is proposed, partly derived from [16], where the reduction of grid injection is the main reason to optimally size the battery (C^i_{bat}).

$$C^i_{bat} = \frac{E^i_{inj} - \frac{(Q^i_{storage,DHW} + Q^i_{storage,SH})}{CoP}}{(SoC_{max} - SoC_{min})\eta_{ch}},$$ (7)

where *CoP* is the mean CoP based on SH and DHW mode, η_{ch} is battery charging efficiency [–], SoC_{max} is the maximum battery State of Charge (SoC) [%] and SoC_{min} is the minimum battery SoC [%].

Please note that the energy storage sizes are based on the equations presented in Section 2.2 and 2.3 of our work.

3. System description

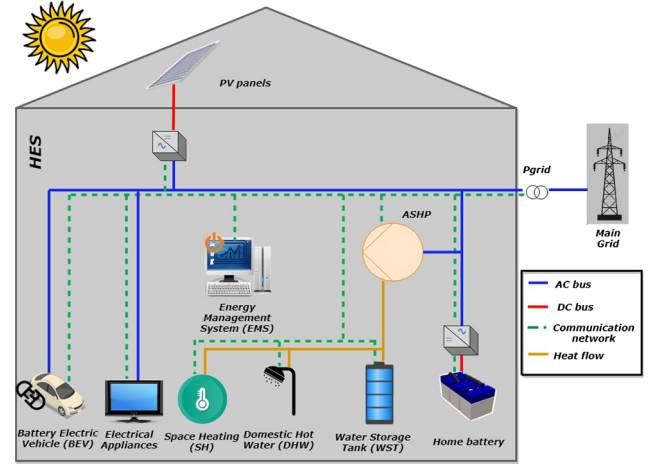HES and CES systems are described in the following sections.

Fig. 1. HES scenario.

3.1. Home energy storage

The home EMS controls the loads of the system by different communication flows between system components (see Fig. 1). The EMS minimizes the amount of electricity taken from the grid by optimizing the utilization of self-produced PV electricity. The electricity (including BEV) and heat demand (provided by an ASHP) of a single household can be satisfied by electricity absorption from the grid, direct consumption of rooftop PV, the battery or the WST (only for heat). The ASHP covers the entire DHW and SH demand of the household. Every household has different demand loads and PV supply. Therefore, the system components are sized individually per household to avoid high investment costs. For HES, we assume that the cost for the capacity of a technology is linear to a certain capacity.

3.2. Community energy storage

CES contains of a number of households, who share a community battery, a community ASHP and a community WST. These are all controlled by a centralized EMS (see Fig. 2). CES consists of larger system components compared to HES due to bigger sized system components. Electricity demand of a specific household can be satisfied by the electricity grid, direct consumption of rooftop PV or by the community battery. Heat demand can be satisfied by the community WST. The localized EMSs control the loads of single households. The community EMS controls the loads of the community system components.

In addition, the electricity utility sends the hourly price and emission signals to the community EMS, so that this data information can be used to schedule flexible loads. Next, this community EMS communicates with the localized EMSs of each households to obtain their demand and PV electricity supply data. After that, the community EMS uses an algorithm to optimize the supply and demand of the community components. A precondition is that the home EMSs can directly interact with the community EMS to communicate on load schedules. Therefore, separate communication lines are required between the community EMS and the home EMSs of the households. We assume that all optimization constraints can be stored and set in the EMSs.

We assume that each household owns a share of the CES system hence their share is allocated and controlled by the community EMS (e.g. see [17]). The community system components are optimally sized for a specified number of households. However, the loads and PV generation differ per household. Consequently, community components are distributed by household shares to divide community costs in a fair way. For instance, community shares of the battery can be obtained from the optimal energy storage capacity sizes (see Eqs. (8) and (9)) of household i.
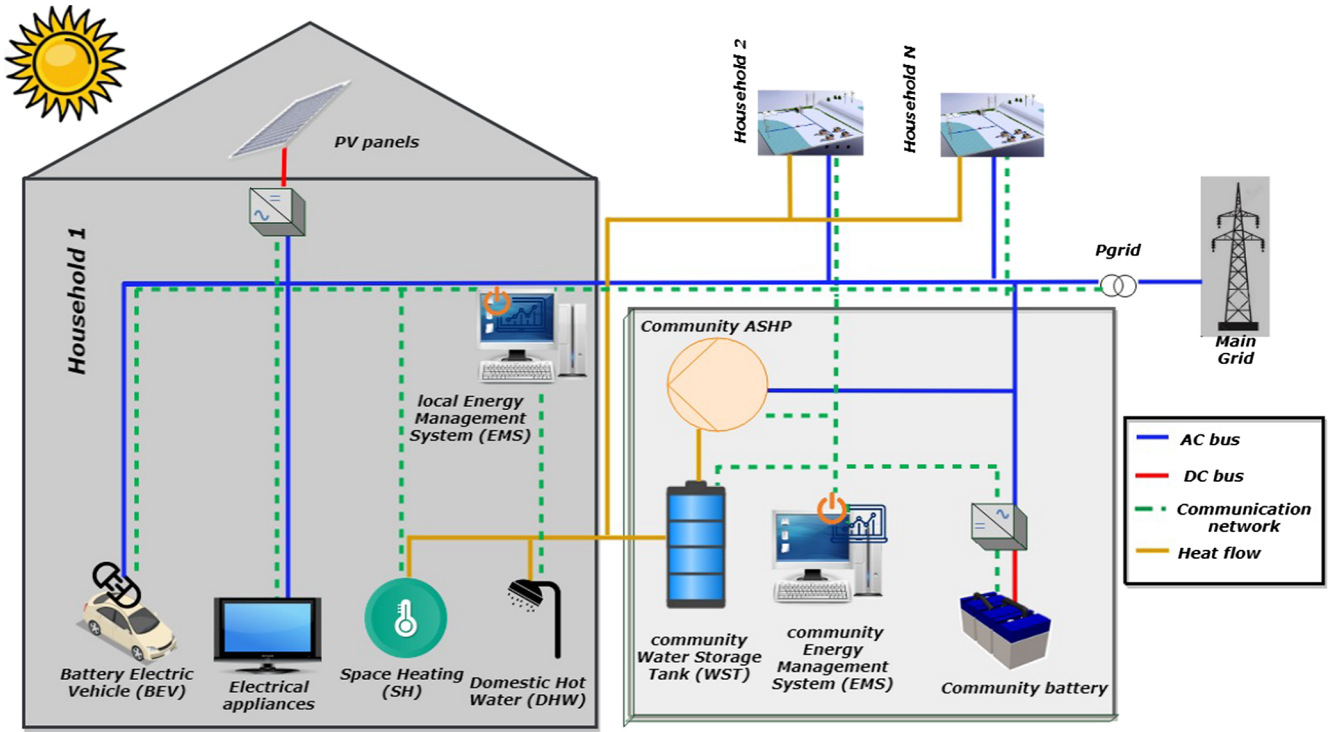
Fig. 2. CES scenario.

When the sum of all individual optimal sizes results in an unrealistically large CES battery size, community shares can be used to determine the allocated storage size in household i. In this way, the allocated community share of each household is multiplied with the CES size. The following equation is proposed to determine the community share of household i (Sb^i) for a system component, derived from [16]:

$$Sb^i = \frac{C^i_{bat}}{\sum\limits_{j=1}^{N} C^j_{bat}}. \tag{8}$$

Alternatively, the following equation is proposed to determine the optimal size of the battery in CES ($Cap_{CES,opt}$) [16].

$$Cap_{CES,opt} = \sum_{i \in N} C^i_{bat}. \tag{9}$$

The above approach (Eqs. (8) and (9)) is also used to size the community WST and the community ASHP. In most cases, larger capacities reduce the costs of storage mediums ($Cost_{sm}$), due to economies of scale from a certain minimum amount of installed power capacity (C_l). For batteries (or battery systems), larger capacities reduce the costs of the balance of plant (power unit), inverter and maintenance [18]. The minimum capacity where economies of scale will start is defined at 10 kW for the power unit in the battery [18]. The cost benefits related to capital investments from the nominal capacity (C_{nom}) are demonstrated in Eq. (10) and is adopted from [14].

$$Cost_{sm} = (\frac{C_{nom}}{C_l})^{0.7} \cdot C_l \cdot cost_{rel}, \tag{10}$$

where $cost_{rel}$ is the relative cost of the technology [euro/kW h].

Also, economies of scale for ASHPs are considered. The UK department of Energy [34] demonstrates average cost reductions of ASHPs of around 12.5 % (i.e. factor of 0.875) per additional kW heat pump installed (with $C_l = 12$ kW heat). The following linear cost equation is proposed to include economies of scale of ASHPs in the CES system ($Cost_{ASHP,CES}$).

$$Cost_{ASHP,CES} = (C_l \cdot cost_{rel}) + (C_{nom} - C_l) \cdot 0.875 \cdot cost_{rel}. \tag{11}$$

Note that no economies of scale are considered for the WST for the economic analysis, since no detailed research is performed on economies of scale of WSTs. Hence we assume that the costs of the WST increase linearly with an increase of the WST capacity.

For a more comprehensive review and additional benefits of CES, we refer to [8]. This system description serves as technology characterization for the optimization model.

4. Optimization model

The main objective of this optimization problem is to minimize both costs and CO_2-emissions during system operation. To achieve this, a multi-objective mixed integer linear programming approach is used. This method has been widely used in the energy field [13,16,17,19,25].

The optimization tool is developed within Python (v 3.6) with data files provided in Excel format. The optimization tool is modeled using Gurobi (v 8.0) software, applied within Python [35]. Each of the case studies are implemented as an optimization problem to calculate the optimal operation costs and CO_2-emissions. Technological trade-offs are optimized from an economic and CO_2-emission perspective under a set of pre-defined constraints, which are based on the system descriptions of Section 3.

4.1. Multi-objective function

The first objective is set to minimize costs of electricity absorbed from the grid ($p^{t,i}_{grid,abs}$), which implies stimulating PVSC since it is assumed that costs of locally produced PV electricity is zero. In addition, grid electricity consumption of households can be shifted to periods when grid electricity prices (c^t) are low (i.e. demand load shifting). Besides costs, the reduction of CO_2-emissions are getting more importance in the assessment of buildings [36,37]. Therefore, a second objective is added to evaluate CO_2-emissions during system operation. This objective is set to minimize grid CO_2-emissions (g^t). This results in the following multi-objective function.

minimize $(f_1(p_{grid,abs}^{t,i})f_2(p_{grid,abs}^{t,i}))$,

where:
$$f_1 = \sum_{t=1}^{T} c^t\, p_{grid,abs}^{t,i}\, \Delta t,$$

$$f_2 = \sum_{t=1}^{T} g^t\, p_{grid,abs}^{t,i}\, \Delta t, \tag{12}$$

where Δt represent the timestep of one hour.

4.2. Constraints

Constraints are applied to let the system operate in a reliable and safe way.

4.2.1. Total balance of system

A system balance is implemented to meet the supply and demand of the state of different variables. At each timeslot t, a power action ($p^{t,i}$) can be expected. This power action could be an interaction with the main grid by absorbing or injecting ($p_{grid,inj}^{t,i}$) power, or with the battery due to charging ($p_{bat,ch}^{t,i}$) or discharging ($p_{bat,dis}^{t,i}$). The power action should be equal to the sum of the shiftable load ($p_{sl}^{t,i}$) and non-shiftable load ($P_{nsl}^{t,i}$), minus the harvested PV generation ($P_{PV}^{t,i}$) in order to ensure the balance between supply and demand of the system. Note that Eqs. (13) and (14) are separated although can be written as one equation.

$$p^{t,i} = (p_{grid,abs}^{t,i} - p_{grid,inj}^{t,i}) + (p_{bat,dis}^{t,i} - p_{bat,ch}^{t,i}), \quad \forall\ i,\ t, \tag{13}$$

where:

$$p^{t,i} = p_{sl}^{t,i} + P_{nsl}^{t,i} - P_{PV}^{t,i}, \quad \forall\ i,\ t. \tag{14}$$

4.2.2. Power boundaries of main grid and battery

Different power boundaries are set to avoid system imbalances. The power absorbed or injected from or to the electricity grid should be less or equal than the maximum allowed amount of power from or to the grid ($P_{grid,max}^i$).

$$0 \leqslant p_{grid,abs}^{t,i} \leqslant P_{grid,max}^i, \quad \forall\ t,\ i, \tag{15}$$

$$0 \leqslant p_{grid,inj}^{t,i} \leqslant P_{grid,max}^i, \quad \forall\ t,\ i. \tag{16}$$

In addition, the charging and discharging power should not exceed the maximum battery charging and discharging power ($P_{bat,max}^i$).

$$0 \leqslant P_{bat,ch}^{t,i} \leqslant P_{bat,max}^i, \quad \forall\ t,\ i, \tag{17}$$

$$0 \leqslant P_{bat,dis}^{t,i} \leqslant P_{bat,max}^i, \quad \forall\ t,\ i. \tag{18}$$

4.2.3. Battery energy storage system

The dynamics of the battery and the related SoC (SoC^{t,i}) can be described by the following equation.

$$SoC^{t,i} = SoC^{t-1,i} - \left(\frac{1}{\eta_{dis} C_{bat}^i}(p_{bat,dis}^{t,i})\Delta t - \frac{\eta_{ch}}{C_{bat}^i}(p_{bat,ch}^{t,i})\Delta t \right), \quad \forall\ t. \tag{19}$$

In addition, the SoC should be within the boundaries of the minimum SoC and maximum SoC of the battery, for functioning purposes and to ensure the lifetime of the battery.

$$SoC_{min} \leqslant SoC^{t,i} \leqslant SoC_{max}, \quad \forall\ t. \tag{20}$$

Also, the SoC at the beginning of the next day should be equal or higher than the SoC at the beginning of the day earlier to ascertain at least an equal charging potential. Note that T represents the time
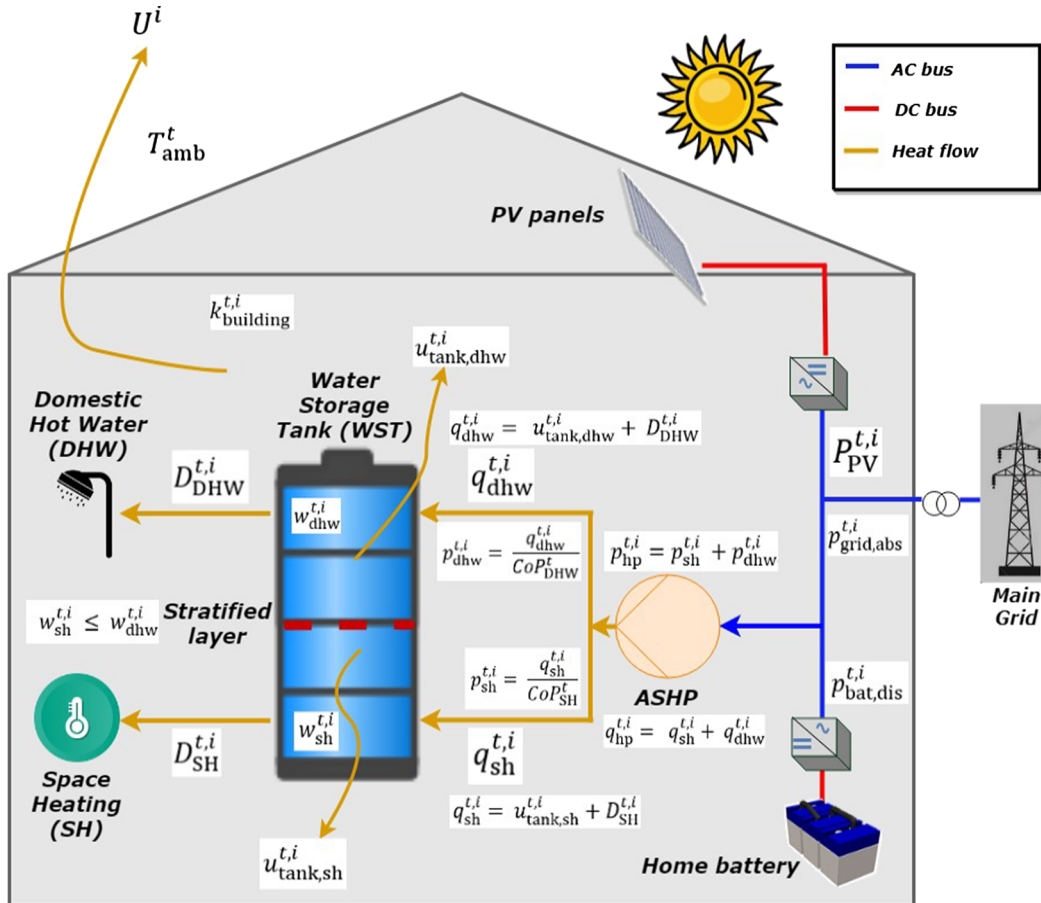

Fig. 3. Heat flows visualized in the HES scenario. Note that electricity flows and other system components are not indicated, on purpose.

horizon (i.e. 24 h in Eq. (21)).

$$\sum_{t=1}^{T} SoC^{t,i} - SoC^{t-1,i} \geqslant 0, \quad \forall\, t. \tag{21}$$

4.2.4. Shiftable devices

Different shiftable loads/devices can be included in the model. However, the only shiftable loads in this model are the BEV and the ASHP. The ASHP can be shifted, but is a special type of shiftable load and is described in Section 4.3.1. Consequently, the following constraints are not applicable to the ASHP. Other shiftable loads can be easily added into the model considering the constraints in this section. Firstly, the total shiftable power demand of a shiftable load a in household i ($p^{a,t,i}$) should meet the daily required amount of energy demand of a (E_{sl}^a).

$$\sum_{t=1}^{T} p^{a,t,i} \Delta t = E_{sl}^a, \quad \forall\, a,\, i. \tag{22}$$

In addition, the demand of all shiftable loads should be equal to the total amount of shiftable power capacity in i at t.

$$\sum_{a=1}^{A^i} p^{a,t,i} = p_{sl}^{t,i}, \quad \forall\, t,\, i. \tag{23}$$

Furthermore, the total power demand can be set to respect the peak power ($P_{peak}^{t,i}$) load to avoid system contingencies.

$$p_{sl}^{t,i} + P_{nsl}^{t,i} \leqslant P_{peak}^{t,i}, \quad \forall\, a,\, i. \tag{24}$$

The power of each shiftable device should be in between the boundaries of the maximum (P_{max}^a) and minimum power (P_{min}^a) the shiftable device can afford to provide a safe operation. Variable "$y^{a,t,i}$" is a binary variable which is activated (e.g. $y^{a,t,i} = 1$) if the load can be used during a specific time.

$$P_{min}^a y^{a,t,i} \leqslant p^{a,t,i} \leqslant P_{max}^a y^{a,t,i}, \quad \forall\, a,\, t,\, i. \tag{25}$$

In addition, the time preference ($TP^{a,t,i}$) of each shiftable device can be set to schedule the shiftable device at a predefined time.

$$y^{a,t,i} \leqslant TP^{a,t,i}, \quad \forall\, a,\, i. \tag{26}$$

4.3. Water storage tank

4.3.1. Air-to-water source heat pump

The ASHP is a special type of shiftable load, and is included into the model to supply SH and DHW demand. ASHPs can offer flexibility and additional benefits, such as the reduction of costs due to demand load shifting by storing heat in a WST [21]. Therefore, the considered system design is based on an ASHP in combination with a WST which can provide some flexibility (i.e. demand load shifting), while considering constraints to ensure user comfort. The heat flows are determined in Fig. 3, to balance heat flows between the WST, ASHP and loads. These heat flows are required for the following constraints.

First of all, the total electricity demand of the ASHP ($p_{hp}^{t,i}$) is the sum of power needed for SH ($p_{sh}^{t,i}$) and DHW ($p_{dhw}^{t,i}$) demand.

$$p_{hp}^{t,i} = p_{sh}^{t,i} + p_{dhw}^{t,i}, \quad \forall\, t,\, i. \tag{27}$$

The following constraint ensures that the total amount of power provided by the ASHP cannot be higher than the maximum installed power of the ASHP.

$$0 \leqslant p_{hp}^{t,i} \leqslant P_{hp,installed}^i, \quad \forall\, t,\, i. \tag{28}$$

Furthermore, the total heat load of the ASHP ($q_{hp}^{t,i}$) contains both heat demand for SH ($q_{sh}^{t,i}$) and DHW ($q_{dhw}^{t,i}$).

$$q_{hp}^{t,i} = q_{sh}^{t,i} + q_{dhw}^{t,i}, \quad \forall\, t,\, i. \tag{29}$$

The authors of [21,38] emphasize the potentially problematic increase of fast ramping rates of heat pumps since this can have a large impact on low-voltage distribution grids. This event can appear when the future penetration of heat pumps is high. Therefore, the following constraint can be implemented to reduce the impact on the electricity grid.

$$P_{ramprate,max}^i \leqslant |p_{hp}^{t,i} - p_{hp}^{t-1,i}|, \quad \forall\, t,\, i, \tag{30}$$

where $P_{ramprate,max}^i$ is the maximum ramp rate the heat pump can operate at in i [kW].

Furthermore, the total heat loss of the WST ($u_{tank}^{t,i}$) contains of the heat loss of WST_{SH} ($u_{tank,sh}^{t,i}$) and the heat loss of WST_{DHW} ($u_{tank,dhw}^{t,i}$).

$$u_{tank}^{t,i} = u_{tank,sh}^{t,i} + u_{tank,dhw}^{t,i}, \quad \forall\, t,\, i. \tag{31}$$

4.3.2. ASHP: SH mode

As mentioned earlier, the ASHP can operate in SH mode and DHW mode. Firstly, the constraints of the SH mode are discussed. The amount of electricity needed for SH, is the SH demand divided by the CoP, specified for SH.

$$p_{sh}^{t,i} = \frac{q_{sh}^{t,i}}{CoP_{SH}^t}, \quad \forall\, t,\, i. \tag{32}$$

The amount of SH demand at t depends on the heat loss of the WST_{SH} ($u_{tank,sh}^{t,i}$) and the SH demand profile ($D_{SH}^{t,i}$). In this case, no flexibility is added for the deviation of inside temperature from the heat demand profile ($D_{SH}^{t,i}$). Alternatively, the model can choose to schedule the SH demand by a decision variable ($u_{sh}^{t,i}$). In this case, the SH demand is generated by multiplying the thermal heat loss of the building (U^i) with the temperature difference between the inside and outside environment at t (see Eq. (33)). This approach can add flexibility to the ASHP by setting the boundaries of the SH demand profile flexibly since the maximum and minimum temperature of the inside building environment ($k_{building}^{t,i}$) can be chosen with Eq. (35). We adopt this approach since this results in a more dynamic and flexible system. Only positive temperature differences are considered, since energy for cooling demand is not included in our work.

$$u_{sh}^{t,i} = U^i (k_{building}^{t,i} - T_{amb}^t), \quad \forall\, t,\, i. \tag{33}$$

The flexible SH supply should be equal to the daily heat demand profile of the household to guarantee sufficient daily SH.

$$\sum_{t=1}^{T} u_{sh}^{t,i} = \sum_{t=1}^{T} D_{SH}^{t,i}, \quad \forall\, t,\, i. \tag{34}$$

However, the above constraints result in an unbounded daily SH demand profile, neglecting the comfort of the residents. Therefore, the following constraint is applied to sustain comfort levels of the residents and ensures that the inside temperature of the building is within the range of predefined minimum ($T_{building,min}^i$) and maximum ($T_{building,max}^i$) inside building temperatures.

$$T_{building,min}^i \leqslant k_{building}^{t,i} \leqslant T_{building,max}^i, \quad \forall\, t,\, i. \tag{35}$$

During most times, the water temperature of WST_{SH} is higher than the inside environment which results in heat losses of the WST_{SH} ($u_{tank,sh}^{t,i}$).

$$u_{tank,sh}^{t,i} = S_{SH} A_{tank} U_{tank} (w_{sh}^{t,i} - k_{building}^{t,i}), \quad \forall\, t,\, i, \tag{36}$$

where S_{SH} is the share of SH of the WST based on volume [–], A_{tank} is the total surface area of the WST [m²], U_{tank} is specific heat loss of the WST [kW m⁻² K⁻¹] and $w_{sh}^{t,i}$ is the water temperature for WST_{SH} at t in i [K].

Furthermore, the daily flexible heat supply of the building and heat loss of WST_{SH} should be equal to the total amount of SH provided by the ASHP.

$$\sum_{t=1}^{T} q_{sh}^{t,i} = \sum_{t=1}^{T} (u_{sh}^{t,i} + u_{tank,sh}^{t,i}), \quad \forall\, t, i. \tag{37}$$

Next, the dynamics of the water temperature in WST_{SH} can be demonstrated by the following constraint. For simplicity, it is assumed that water flows are the same at every place of the system.

$$w_{sh}^{t,i} = w_{sh}^{t-1,i} + \frac{(q_{sh}^{t,i} - u_{tank,sh}^{t,i} - u_{sh}^{t,i})\Delta t}{c\, C_{SH,tank}^{i}}, \quad \forall\, t, i, \tag{38}$$

where $C_{SH,tank}^{i}$ is mass of storage capacity for SH in i [kg].

The following constraint ensures that the water temperature inside the WST_{SH} will be in the range of predefined minimum ($T_{SH,min}^{i}$) and maximum ($T_{SH,max}^{i}$) water temperatures.

$$T_{SH,min}^{i} \leqslant w_{sh}^{t,i} \leqslant T_{SH,max}^{i}, \quad \forall\, t, i. \tag{39}$$

The following constraint ensures that the supply water temperature inside the WST_{SH} equals or is higher than the minimum required supply temperature for the distribution system ($T_{supply,min,SH}^{i}$, determined by Eq. (6)) to provide sufficient SH during cold days.

$$w_{sh}^{t,i} \geqslant T_{supply,min,SH}^{t}, \quad \forall\, t, i. \tag{40}$$

4.3.3. ASHP: DHW mode

The DHW mode is essential to supply hot tap water. Again, the electricity load is the heat supplied by the ASHP divided by the CoP, specified for DHW.

$$p_{dhw}^{t,i} = \frac{q_{dhw}^{t,i}}{CoP_{DHW}^{t}} \quad \forall\, t, i. \tag{41}$$

DHW demand ($D_{DHW}^{t,i}$) is indicated as inflexible load. However, the WST delivers flexibility. The total amount of daily DHW heat supplied by the ASHP should be equal to the daily DHW demand and heat loss of the WST_{DHW} ($u_{tank,dhw}^{t,i}$).

$$\sum_{t=1}^{T} q_{dhw}^{t,i} = \sum_{t=1}^{T} (D_{DHW}^{t,i} + u_{tank,dhw}^{t,i}), \quad \forall\, t, i. \tag{42}$$

The heat loss of WST_{DHW} is calculated in the same way as with SH mode.

$$u_{tank,dhw}^{t,i} = S_{DHW} A_{tank} U_{tank} (w_{dhw}^{t,i} - k_{building}^{t,i}), \quad \forall\, t, i, \tag{43}$$

where S_{DHW} is the share of DHW of the WST_{DHW} based on volume [–] and $w_{dhw}^{t,i}$ is water temperature for WST_{DHW} at t in i [K].

The dynamics at the next t of WST_{DHW} is modelled in the same way as with WST_{SH} mode, where $C_{DHW,tank}^{i}$ represents the mass of the water in WST_{DHW}.

$$w_{dhw}^{t,i} = w_{dhw}^{t-1,i} + \frac{(q_{dhw}^{t,i} - u_{tank,dhw}^{t,i} - u_{dhw}^{t,i})\Delta t}{c\, C_{DHW,tank}^{i}}, \quad \forall\, t, i. \tag{44}$$

In addition, the water temperature of WST_{DHW} cannot be higher or lower than predefined upper and lower water temperature limits.

$$T_{DHW,min}^{i} \leqslant w_{dhw}^{t,i} \leqslant T_{DHW,max}^{i}, \quad \forall\, t, i. \tag{45}$$

Finally, the following constraint ensures that the water temperature in WST_{DHW} is higher than WST_{SH}, so that the water is divided in stratified layers.

$$w_{sh}^{t,i} \leqslant w_{dhw}^{t,i}, \quad \forall\, t, i. \tag{46}$$

4.4. Additional constraints for CES

For the CES scenario, some constraints are modified since system components can be based on community shares. All earlier constraints also apply to CES, unless described otherwise in this section. The battery capacity of household i in CES ($C_{bat,CES}^{i}$) can be calculated by

multiplying the battery share with the total capacity of the battery in CES (Cap_{CES}).

$$C_{bat,CES}^{i} = Sb^{i} Cap_{CES}. \tag{47}$$

The SoC of battery is slightly modified since the SoC is based on battery shares [16].

$$SoC^{t,i} = SoC^{t-1,i} - \left(\frac{1}{\eta_{dis} C_{bat,CES}^{i}} (p_{bat,dis}^{t,i})\Delta t - \frac{\eta_{ch}}{C_{bat,CES}^{i}} (p_{bat,ch}^{t,i})\Delta t \right), \quad \forall\, t. \tag{48}$$

Furthermore, the following constraints are implemented to ensure that the battery power is lower than the maximum allowed of power the cables can afford.

$$0 \leqslant p_{bat,ch}^{t,i} \leqslant Sb^{i} P_{bat,max}, \quad \forall\, t, \tag{49}$$

$$0 \leqslant p_{bat,dis}^{t,i} \leqslant Sb^{i} P_{bat,max}, \quad \forall\, t. \tag{50}$$

Additionally, the community ASHP and WST are distributed according to their heat demand share, using the same methodology (i.e. Eq. (47)).

5. Performance indicators

Performance indicators are essential to assess the system performance of alternatives and a baseline scenario (see Section 6.1 for the baseline scenario). Firstly, the optimization model gives an optimization based on operation costs and CO_2-emissions per assessment period (here assumed to be one year, i.e. 8760 h with Δt representing one hour). Note that injected PV electricity is remunerated with the wholesale electricity price at t (c_{we}^{t}). Furthermore, we assume that electricity generation (i.e. grid CO_2-emissions) is avoided when electricity is injected into the electricity grid hence a second term is added to Eq. (52).

$$c_{annual}^{i} = \sum_{t=1}^{8760} (c^{t} p_{grid,abs}^{t,i} - c_{we}^{t} p_{grid,inj}^{t,i})\Delta t, \tag{51}$$

$$g_{annual}^{i} = \sum_{t=1}^{8760} (g^{t} p_{grid,abs}^{t,i} - g^{t} p_{grid,inj}^{t,i})\Delta t, \tag{52}$$

where c_{annual}^{i} are the annual operation costs for system operation in i [euro/year] and g_{annual}^{i} are the annual CO_2-emissions for system operation in i [kg CO_2-eq./year].

5.1. PVSC

The main goal of the optimization model is to minimize electricity consumption from the grid, by maximizing the consumption of self-produced PV electricity during system operation. Consequently, the PVSC ratio is essential to compare different alternatives on the ability to consume self-produced PV generation. PVSC is always between 0 and 1, and closer to 1 means a higher self-consumption in i ($PVSC^{i}$).

$$PVSC^{i} = \frac{\sum_{t=1}^{8760} (P_{PV}^{t,i} - p_{grid,inj}^{t,i})}{\sum_{t=1}^{8760} P_{PV}^{t,i}}. \tag{53}$$

5.2. Economic performance indicators

We consider investment, installation and maintenance costs for all devices (battery, ASHP, WST and PV panels). A more detailed overview of the techno-economic data can be found in Appendix A. The following economic indicators are used.

5.2.1. Scenario I: HES

With the Levelized Costs of Electricity (LCOE), the average cost per unit electricity delivered to the end-user customer is determined, which includes both PV and grid electricity. This indicator evaluates alternatives on the price of electricity based on investments (I_{HES}), annual maintenance costs ($c_{maintenance}^i$) and annual operation costs.

$$\text{LCOE}^i = \frac{I_{HES} + \sum_{l=1}^{L} (c_{annual}^i + c_{maintenance}^i)/(1 + \gamma)^l}{\sum_{l=1}^{L} (\sum_{t=1}^{8760} (p_{sl}^{t,i} + P_{nsl}^{t,i})/(1 + \gamma)^l)},$$

(54)

where LCOE^i are the levelized costs of electricity in i [euro/kW h], γ is the interest rate [%] and L is the lifetime of the system [years].

The simple Pay Back Period (PBP) is used to determine the number of years before the initial investment in HES is recovered in i (PBP_{HES}^i).

$$\text{PBP}_{HES}^i = \frac{I_{HES}}{R^i},$$

(55)

where R^i is the cost reduction compared to a reference scenario due to the reduction of energy absorbed from the power and gas grid [euro].

5.2.2. Scenario II: CES

The same equation is used to calculate the LCOE in CES, with a compensation for the investment with the community share size.

$$\text{LCOE}^i = \frac{Sb^i I_{CES} + \sum_{l=1}^{L} (c_{annual}^i + c_{maintenance}^i)/(1 + \gamma)^l}{\sum_{l=1}^{L} (\sum_{t=1}^{8760} (p_{sl}^{t,i} + P_{nsl}^{t,i})/(1 + \gamma)^l)},$$

(56)

where I_{CES} are the investment costs in CES [euro].

Again, the simple PBP is used to determine the number of years before the initial investment in CES is recovered for household i (PBP_{CES}^i).

$$\text{PBP}_{CES}^i = \frac{Sb^i I_{CES}}{R^i}.$$

(57)

5.3. Environmental performance indicators

The most commonly used method to determine the environmental performance of products and systems over their entire lifetime is the LCA framework [39]. The strength of an LCA is that it includes all environmental-relevant flows, such as emissions, energy, materials, natural resources and waste, of a process or product. LCA is shaped by the series of international standards called ISO 14040-14043. According to ISO 14040, an LCA contains of four steps: goal and scope definition, inventory analysis, Life Cycle Impact Assessment and interpretation of the results [40,41].

The ecoinvent (v3.4) database is used for data collection of LCA processes with the system model "Allocation, cut-off by classification" [42]. The IPCC 2013 method is adopted to indicate the amount of Global Warming Potential, and focuses on greenhouse-gas emissions which is in kg CO_2-equivalent [43,44]. From now on, all greenhouse-gas emissions are included when we refer to CO_2-emissions, since Global Warming Potential is in CO_2-equivalent. Other environmental burdens are out of the scope of this research. In addition, the operation and production phase of system components are considered in LCA foreground processes. End-of-life burdens are only considered in background LCA processes. End-of-life is not included in LCA foreground processes, due to the complexity of the end-of-life phase of batteries [45] and other system components.

5.3.1. Avoided carbon emissions during lifetime

The amount of avoided CO_2-emissions during the system lifetime ($CO_{2\ avoided}^i$) can be calculated by determining the CO_2-emissions of the baseline scenario during lifetime ($CO_{2\ baseline}^i$) reduced by the CO_2-emissions of the analyzed HES or CES alternative during lifetime ($CO_{2\ alternative}^i$).

$$CO_{2_{avoided}}^i = CO_{2_{baseline}}^i - CO_{2_{alternative}}^i.$$

(58)

5.3.2. Carbon intensity of electricity delivered

Alternatively, the following equation is used to compare the carbon intensity (G) during the system lifetime of alternatives per unit electricity delivered.

$$G = \frac{CO_{2_{alternative}}^i}{\sum_{l=1}^{L} \sum_{t=1}^{8760} (p_{sl}^{t,i} + P_{nsl}^{t,i})}.$$

(59)

6. Data: swiss case study

We limit our assessment to the PVSC application since there is no feed-in tariff available for small PV installations (2–10 kW$_p$) in Switzerland [7,46]. The optimization model is applied on the "Flexi" project in the village Cernier. Cernier is situated in the North-West of Switzerland in the Swiss canton Neuchâtel at an altitude of 820 m and is populated by 2200 citizens. We assume that Cernier is a representative Swiss case study in terms of PV yield and heating degree days. The primary objective of Flexi is to shift electricity consumption of households towards PV generation time, to reduce the mismatch between electricity consumption and PV electricity generation. The selected households are divided into three groups to examine the potential of demand load shifting with different measurements [47].

For our paper, we select the control group "0" since we assume that this sample is not influenced by measures. Group "0" contains of 22 households. The year 2014–2015 (i.e. 1st of January 2014 until 31th of December 2014) is chosen as assessment period. Hourly ambient temperatures are derived from MeteoSwiss [48] and are based on hourly temperature profile data of the meteorological weather station located in Chaumont. This station is situated 6 km from Cernier and is approximately located at the same altitude. Therefore, we assume that it represents the same climate conditions as in Cernier.

Heat loss (i.e. U-value) data is obtained from the authors of [49] to acquire household SH demand. They have presented typical heat loss values for Swiss buildings. From the total of 22 households, we assume that the first 10 households have a thermal heat loss value of an average Swiss building with U^i-values of 0.10 kW/K. The next 6 households have a thermal heat loss value which correspond to a less insulated building, with U^i-values of 0.15 kW/K. We assume that the building envelope of the other 6 households are better insulated, with U^i-values of 0.07 kW/K. The annual heat demand for DHW is indicated as 1060 kW h heat per household [50]. Daily DHW and SH profiles are obtained from the Swiss Times Energy system Model [51].

PV generation is modelled within Python with the pvlib package [52]. The PV technology is based on the PV technology which has the highest market share today, which are multi-Si modules [9]. Irradiance data, wind speed and temperature data at hourly resolution are obtained from MeteoSwiss for the year 2014–2015 [48]. The performance of PV modules under different weather conditions (e.g. temperatures) is considered. We assume an average rooftop PV surface area available of 19.6 m^2 per household [53]. Other techno-economic data can be found in Appendix A.

Furthermore, we assume that the PV panels are installed on a surface tilt of 30°. Approximately optimal surface solar conditions are considered with a surface azimuth angle of 180° for the first 4 households. Variation between households is generated by different surface azimuth angles of the installed solar panels of 180° (south oriented), 90° (east-oriented) and 270° (west-oriented) on different households.

The NREL"s PV Watts model is used in the pvlib package in Python to determine AC power, with a nominal efficiency of the inverter of 96% [54].

In our paper, a time-of-use price scheme is considered since most Swiss electricity suppliers offer such a price scheme [55]. The price scheme is specified for Cernier, where a high electricity price tariff is applied from 7.00–21.00. The electricity price is specified on 0.183 euro/kW h during these times. The low electricity price is applied during other times (night) and is specified on 0.101 euro/kW h [56].

Hourly CO_2-emissions are derived from Swiss Times Energy system Model,[1] where the hourly dispatch of electricity generation units is simulated for different weekdays, weekend-days and seasons for Switzerland [57]. An LCA approach is used to determine hourly carbon intensity by using the hourly share of generation units and multiply these with the LCA emissions factors of electricity generation units. LCA emission factors are based on the ecoinvent 3.4 database and the IPCC (2013) Life Cycle Impact Assessment methodology. Net imports from neighbouring countries are included to determine the average import emission factor. The imports shares are based on the total annual imports for the year 2014–2015 from Austria (20.8%), Germany (40.8%), France (35.5%) and Italy (2.9%) [58].

6.1. Model input parameters

The multi-objective function is set to give equal importance to costs and CO_2-emissions (see Table 1 for configurations), for the reason mentioned in Section 4.1. We decide to neglect the trade-off between the individual optimization of costs or CO_2-emissions in this paper, since we aim to focus on economic feasibility in combination with a good environmental performance. A lithium-ion-battery is considered with a Nickel-Manganese-Cobalt oxide (NMC) cathode as described in the work of [23,59]. NMC lithium-ion-batteries are widely used in stationary battery applications [60], such as the Tesla Powerwall [61]. The battery is designed to provide a power to storage ratio of 1:2 ($P_{bat,max}^i/C_{bat}^i$). The system lifetime is set to 20 years, which is the lifetime of the power unit of the battery [23], the ASHP and the WST.

We specify the limits of the inside temperatures of the building between 292 K and 294 K for comfort purposes. The WST contains of two storage layers. The temperature limits of WST_{SH} are specified between 303 and 323 K. The temperature limits of WST_{DHW} are indicated between 313 and 333 K [30].

Next, the BEV is considered as shiftable load and can be scheduled between 19.00 and 7.00 during weekdays. During weekends, the BEV can be charged during the entire day since we assume that the residents are at home. Additionally, we assume that the residents drive 37 km per day, which is the average daily travelling distance in Switzerland [62]. This results in a daily BEV charging demand of 7.18 kW h per household. We assume that each household owns one BEV since it is expected that the future penetration of BEVs will be high [63].

Furthermore, the EMS has perfect knowledge on demand loads, PV generation and CoP prediction over one year. This assumption is reasonable since the main purpose of this paper is to evaluate annual system costs and CO_2-emissions. The maximum amount of injected and absorbed grid electricity ($P_{grid,max}^i$) is designed to absorb the maximum individual electricity demand peak of a household in the community (i.e. 8 kW). The maximum power peak ($P_{peak}^{t,i}$) is set at 12 kW to avoid system contingencies.

To examine different alternatives, a baseline scenario is developed, which corresponds to a typical household in Switzerland. The energy consumption of the baseline scenario contains of electricity supplied by the electricity grid and heat demand supplied by natural gas (with 87%

---

[1] The year 2010 is used as assessment year for CO_2-emissions since the year 2014 is not available in the used version of the Swiss Times Energy system Model.

Table 1
Configurations of alternatives.

	HES_{std} HES_{opt} CES_{opt}	
Battery energy storage system		
$P_{grid,max}^i$	8	[kW]
SoC_{min}	3.5	[%]
SoC_{max}	96.5	[%]
SoC_0	50	[%]
$\eta_{ch} = \eta_{dis}$	0.943	[–]
$P_{bat,max}^i : C_{bat}^i$	1:2	[–]
$T_{building,min}^i$	292	[K]
$T_{building,max}^i$	294	[K]
$P_{ramprate,max}^i$	2	[kW]
U_{tank}	0.548	[W m^{-2} K^{-1}]
Water storage tank		
$T_{SH,min}^i$	303	[K]
$T_{SH,max}^i$	323	[K]
$T_{DHW,min}^i$	313	[K]
$T_{DHW,max}^i$	333	[K]
Grid		
$P_{peak}^{t,i}$	12	[kW]
Battery electric vehicle		
P_{min}^a	0	[kW]
P_{max}^a	1.4	[kW]

efficiency of gas heating [57]). A flat electricity price of 0.182 euro/kW h [56] and a gas price of 0.08 euro/kW h heat are used for the baseline scenario [64]. In Switzerland, residential households can receive a subsidy of their PV investment with a maximum coverage of 30% of their PV investment [46]. Therefore, a subsidy for the installment of PV generation (30% reduction of total PV investment) is included in the economic analysis.

Three alternative system configurations are proposed. Firstly, a HES system (HES_{std}) where each household owns a standardized battery size (i.e. same storage capacity as the Tesla Powerwall 2 of 13.5 kW h), a WST_{SH} (sized with Eq. (5) and a same sized WST_{DHW} (sized with Eq. (3)). For HES_{std}, the battery is non-optimally sized. These sizing decisions are reasonable since households often get the same system configuration installed for cost reasons. However, the work of [16] demonstrates that optimal sizing of batteries could reduce costs significantly. Therefore, a second HES system (HES_{opt}) is examined, where the battery is optimally sized per household using Eq. (7). Lastly, a CES scenario (CES_{opt}) is developed where the battery is optimally sized per household to assess the difference in lifetime performance between HES and CES systems. Furthermore, we assume that the storage capacity should be able to store 90% of the time the daily grid injection (i.e. E_{inj}^i) of household i in both the HES_{opt} and CES_{opt} alternatives. Table 1 shows the described input parameters which are the same for all alternatives for each household. Other techno-economic data can be found in Appendix A.

6.2. Sensitivity analysis

6.2.1. Trade-off between electricity storage and heat storage

The sizing of the WST_{SH} is based on a static equation presented in [32], where the annual heat peak demand of a specific household is multiplied with a static value (parameter $V_{SH,Qpeak}$, which is 20 l kW^{-1}). However, it can be expected that a larger WST_{SH} results in lower investment costs since the storage medium costs of a WST (120 euro/kW h heat storage [32]) is lower compared to a NMC battery (991 euro/kW h electricity storage, including the power system [23]). Therefore, the sizes of the WST_{SH} and battery are varied in the sensitivity analysis.

Parameter $V_{SH,Qpeak}$ is varied from 10 until $500\,l\,kW^{-1}$ to examine the effect of larger WST sizes on economic indicators. In the case of a negative battery capacity, the battery capacity is set back to $0\,kW\,h$ to prevent model errors.

7. Results

The following section discusses the results from the optimization model. Firstly, annual results are explained. After that, a weekly household operation for the HES$_{opt}$ alternative is demonstrated to serve as an example. Thirdly, the results of the economic and environmental analysis are presented. Lastly, the results from the sensitivity analysis are provided.

7.1. System configurations and annual results

Table 2 demonstrates the average annual values of 22 households in Cernier. Lower community battery capacities are obtained from the HES$_{opt}$ and CES$_{opt}$ alternatives in comparison with the HES$_{std}$ alternative. This can be explained due to the optimally sized battery capacity in HES$_{opt}$ and CES$_{opt}$. While with the HES$_{std}$ alternative, a standardized storage capacity (i.e. $13.5\,kW\,h$) has been installed. Note that the in- and outputs of HES$_{opt}$ and CES$_{opt}$ are the same since these two alternatives are sized with the same sizing methodology (i.e. Eq. (7)).

It turns out that HES$_{opt}$ and CES$_{opt}$ have slightly lower PVSC values (0.981 vs. 0.992), battery charge and discharge throughputs in comparison with HES$_{std}$. This can be explained due to the smaller battery size in HES$_{opt}$ and CES$_{opt}$. Furthermore, HES$_{std}$ shows slightly lower grid injection and higher grid absorption values since a larger battery is able to store and shift more of the self-produced PV electricity.

7.2. Single household operation

7.2.1. Winter week

From Fig. 4, it turns out that the EMS choose to absorb grid electricity when grid electricity prices and CO_2-emissions are low (i.e. mostly during late evening and midnight) in order to reduce operation costs and grid CO_2-emissions. Logically, battery charging follows the same pattern as grid electricity absorption. Please note that in Fig. 4 and 6 "P_{bat}" only represents battery charging, hence the SoC is increased when the battery is charged. No electricity is injected in the grid during this winter week as a result of low solar irradiation. Furthermore, Fig. 4 demonstrates that the lower and upper limit of the battery SoC are respected, which are 3.5% and 96.5%, respectively. The SoC of the battery logically follows the same pattern as battery charging. The SoC clearly indicates that the battery is extensively used since the battery is entirely discharged on a daily basis during this winter week. The BEV charging shows the same pattern as grid electricity absorption. This is reasonable, since the BEV can be charged during the late evening and during midnight, when grid electricity prices and CO_2-emissions from the grid are relatively low.

Fig. 5 demonstrates that inside building temperatures fluctuate during the day, but remain within the comfort range of inside temperatures. This fluctuation can be explained by the heat loss of the building and the (partly) flexible heat supply of the ASHP. Furthermore, this figure demonstrates that the EMS shifts the heat generation of the ASHP towards times when electricity prices and CO_2-emissions from the grid are low and during times with PV supply, since the electricity price is assumed to be zero of self-generated PV power. At certain times, the peak power of the ASHP is reached as a result of SH demand and demand load shifting. From these fluctuations, it becomes evident that the storage size of the WST$_{SH}$ is relatively small (i.e. $85\,l$ for this household) compared to the SH load. The minimum required water temperature of WST$_{SH}$ ($T^i_{supply,min,SH}$) for the heating distribution system slightly increases during this winter week as a result of lower outside temperatures later this week, see Appendix B.

7.2.2. Summer week

In this section, only differences between the winter week and summer week are discussed. Fig. 6 illustrates more PV generation in comparison with the winter week due to higher solar irradiation. Consequently, less electricity is absorbed from the electricity grid since the battery is also charged during day times with self-produced PV electricity. Also, the SoC fluctuations reveal that the depth of discharge of the battery is smaller compared to the winter week. This can be explained by higher PV generation and less need to charge or discharge the battery with grid electricity, to avoid high costs and CO_2-emissions from the grid. During weekends, the BEV can be charged during day times. This event is clearly visualized on the 27th of July, where the BEV is partly charged during day time with self-produced PV electricity.

Fig. 7 demonstrates that the ASHP requires less electricity due to lower heat loss of the building, as a result of higher outside temperatures. This pattern is also visualized within the WST, where less fluctuations of water temperatures are demonstrated. At certain times with high PV generation, the WST and battery are fully charged (e.g. around noon at the 24th and 25th of July). Consequently, PV electricity must be injected into the electricity grid.

Table 2
Average annual values of the community of storage capacity of WST and battery, grid operations and PVSC.

|	Annual average	Baseline	HES$_{std}$	HES$_{opt}$ and CES$_{opt}$	
Model input	District battery capacity	0	297	203	[kW h]
	Average capacity	0	13.5	9.2	[kW h]
	$P^i_{bat,max}$	0	6.8	4.6	[kW]
	Annual PV production	0	3075	3075	[kW h]
	$Q^i_{WST,SH}$	0	2.05	2.05	[kW h heat]
	$Q^i_{WST,DHW}$	0	3.06	3.06	[kW h heat]
	$P^i_{hp,installed}$	0	1.70	1.70	[kW]
	Electricity demand	5384	5384	5384	[kW h]
	Heat demand	12,561	12,561	12,561	[kW h heat]
Model output	Power demand	5384	9227	9229	[kW h]
	Gas demand	14438	0	0	[kW h heat]
	Battery charge	0	3524	2882	[kW h]
	Battery discharge	0	3142	2569	[kW h]
	Grid absorption	0	6558	6525	[kW h]
	Grid injection	0	25	58	[kW h]
	PVSC	–	0.992	0.981	[–]
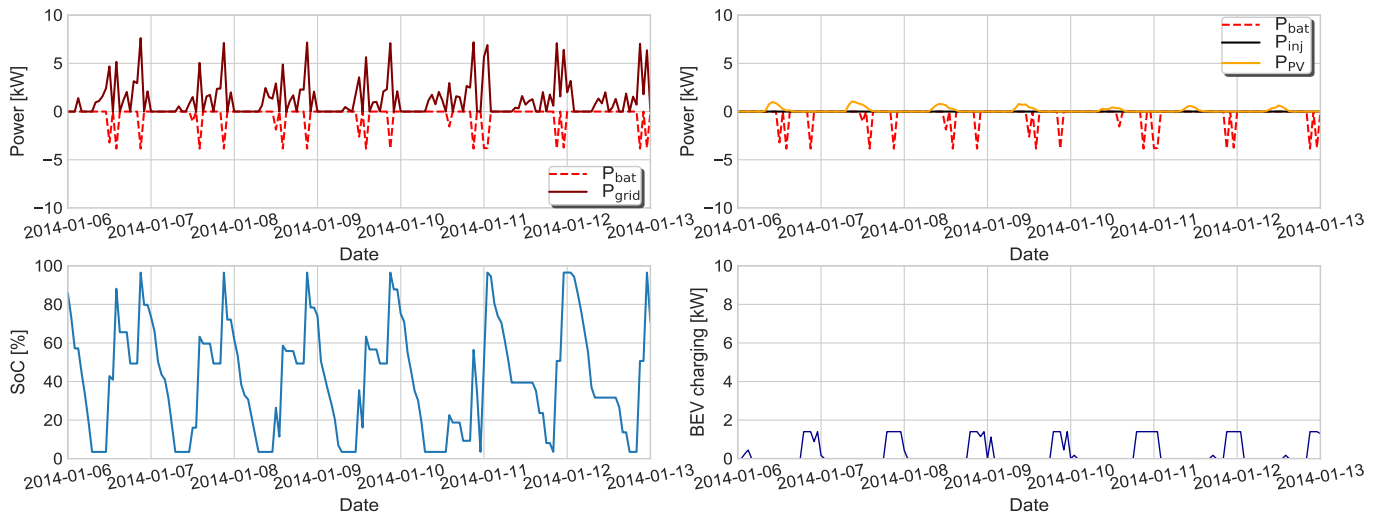
Fig. 4. Single household operation during a winter week for the battery, PV generation and BEV.

7.3. Economic analysis

Table 3 shows the results of the economic analysis. All three alternatives demonstrate lower operational (electricity) costs compared to the baseline scenario since the EMS choose to shift the electricity demand to times when electricity prices and CO_2-emissions are low. The system operation performance is comparable between the three alternatives. HES_{std} has slightly lower costs during system operation than HES_{opt} and CES_{opt}, which is reflected in lower annual electricity costs. This can be explained due to the bigger battery size in HES_{std} (13.5 kW h vs. 9.2 kW h in HES_{opt} and CES_{opt}) since this reduces the absorption of grid electricity hence reduces annual costs.

However, the differences between the operation costs of HES_{opt}/CES_{opt} (807 euro/year) and HES_{std} (802 euro/year) are small. This demonstrates that HES_{std} cannot profit sufficiently from the larger battery capacity since HES_{std} scores worse on the PBP (35.5 years) and LCOE (0.401 euro/kW h electricity).

CES_{opt} performs best on both PBP and LCOE, followed by HES_{opt} and HES_{std}, respectively. However, CES_{opt} has a higher PBP (21.2 years) than the system lifetime (20 years), which means that all alternatives are non-profitable at this moment. The comparatively good performance of CES_{opt} can be explained by economies of scale and due to the optimally sized storage capacity of the battery. The investment costs of CES_{opt} and HES_{opt} are lower compared to HES_{std} due to the smaller battery sizes in these alternatives.

At the moment, battery costs are still high (991 euro/kW h electricity storage [23]) and this has a large impact on the economic results. Another economic influencer is the investment of the ASHP, which covers a significant part (approximately 30%) of the total investment costs.

7.4. Environmental analysis

From Table 4, it turns out that each system design reduce CO_2-emissions compared to the baseline scenario, with more than 61 ton CO_2-eq. during system lifetime. The differences between the three alternatives correspond to the economic performance indicators. The annual CO_2-emissions of HES_{opt} and CES_{opt} are slightly higher compared to HES_{std}, due to a lower PVSC which results in a higher amount of carbon-intensive grid absorption. However, CO_2-intensity during the system lifetime is the lowest for CES_{opt}. This can be explained by its lower battery capacity and its beneficial economies of scale during the production phase, since battery production is a carbon-intensive activity. Again, CES_{opt} performs slightly better than HES_{opt} due to economies of scale, since a larger sized WST and battery results in less carbon-intensive production of these system components.
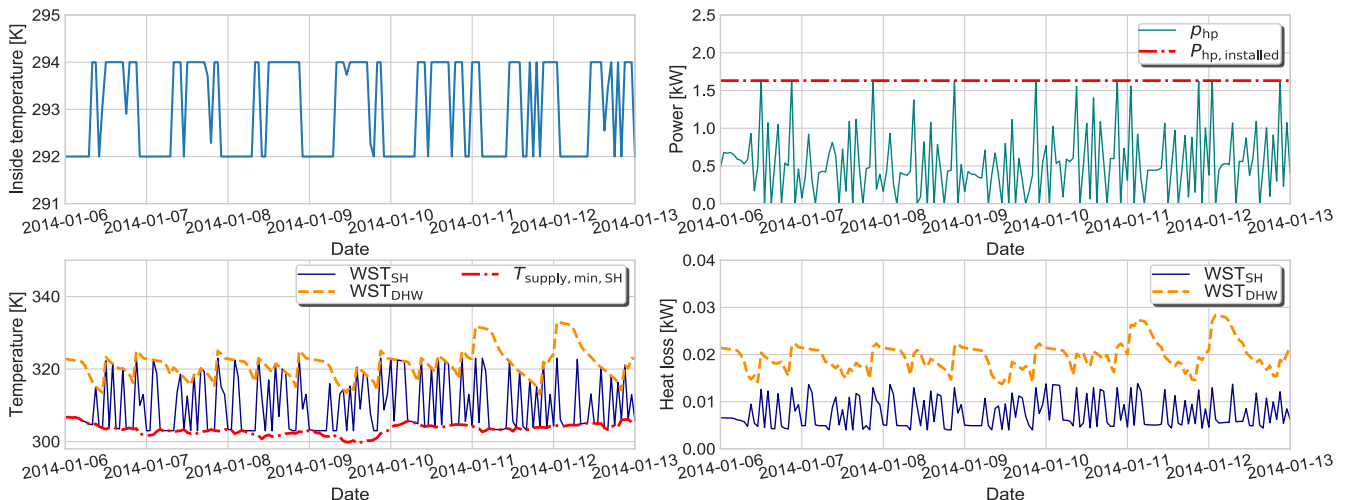

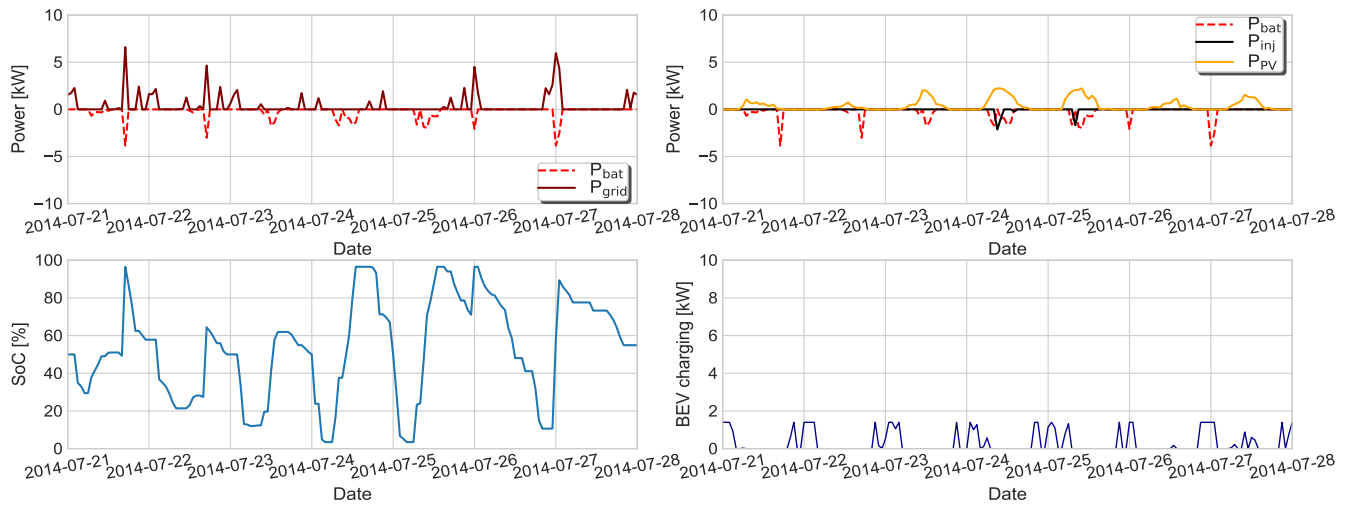**Fig. 5.** Single household operation during a winter week for the ASHP and WST.

Fig. 6. Single household operation during a summer week for the battery, PV generation and BEV.

7.5. Sensitivity analysis

7.5.1. Comparison of battery vs. WST capacity

Fig. 8 and 9 demonstrate the trade-offs between battery capacity, WST capacity, PBP, PVSC and the economic break-even point of the CES_{opt} and HES_{opt} alternatives. For both alternatives, the reduction of the battery capacity results in significantly lower PBPs since battery costs (991 euro/kW h electricity storage) are comparably higher than WST costs (120 euro/kW h heat storage).

In addition, these figures demonstrate that economic feasibility can be reached for both the CES_{opt} and HES_{opt} alternatives. For CES_{opt}, when the battery share size is decreased to 7.4 kW h and the heat storage size in WST_{SH} is increased to approximately 8 kW h per household (i.e. a WST_{SH} of 350 l). At this point, the PBP is lower than the system lifetime (i.e. 20 years). In this way, the battery in CES must be reduced to a size of 163 kW h electricity storage. Furthermore, the HES_{opt} alternative shows an economic profitable system design when the battery size is decreased to approximately 1.8 kW h electricity storage and the WST_{SH} size is increased to 30 kW h heat storage (i.e. a WST_{SH} of 1300 l) per household. However, the PVSC of HES_{opt} (PVSC of 0.905) is less beneficial than CES_{opt} (PVSC of 0.973) when a profitable system design is reached, since the larger battery in CES_{opt} is able to store a larger amount of self-produced PV electricity.

Furthermore, the PVSC rates of both systems are reduced when the battery capacity is decreased. This can be explained by the proposed

Table 3
Results on economic performance indicators: annual electricity costs, annual costs and annual savings. Note that the LCOE and PBP are based on the system lifetime. These numbers represent the average costs of a household and investments includes all implemented electric devices in a household.

	Baseline	HES_{std}	HES_{opt}	CES_{opt}	Unit
I_{HES}/Sb^fI_{CES}	0	34085	27009	20289	[Euro]
Electricity costs	0.182	0.121	0.123	0.123	[Euro/kW h]
Annual costs[a]	2109	802	807	807	[Euro/year]
Annual savings[b]	0	46.2	46.1	46.4	[%]
LCOE ($\gamma = 4\%$)	0.182	0.401	0.348	0.290	[Euro/kW h]
PBP	0	35.5	28.6	21.2	[Years]

[a] Baseline consists of electricity (979 euro/year) and gas costs (1130 euro/year), alternatives only have electricity costs (operation costs are not included in annual costs).
[b] The relative annual savings are calculated by dividing the annual savings of an alternative with the annual costs of the baseline scenario. Note that operation costs are included.

system design, where the heat stored in the WST cannot be regenerated into electricity. In this way, the PVSC is a good indicator on the quality of energy storage. This indicates that battery storage has a higher storage quality compared to WST, since the battery can supply both energy for heat and electricity.
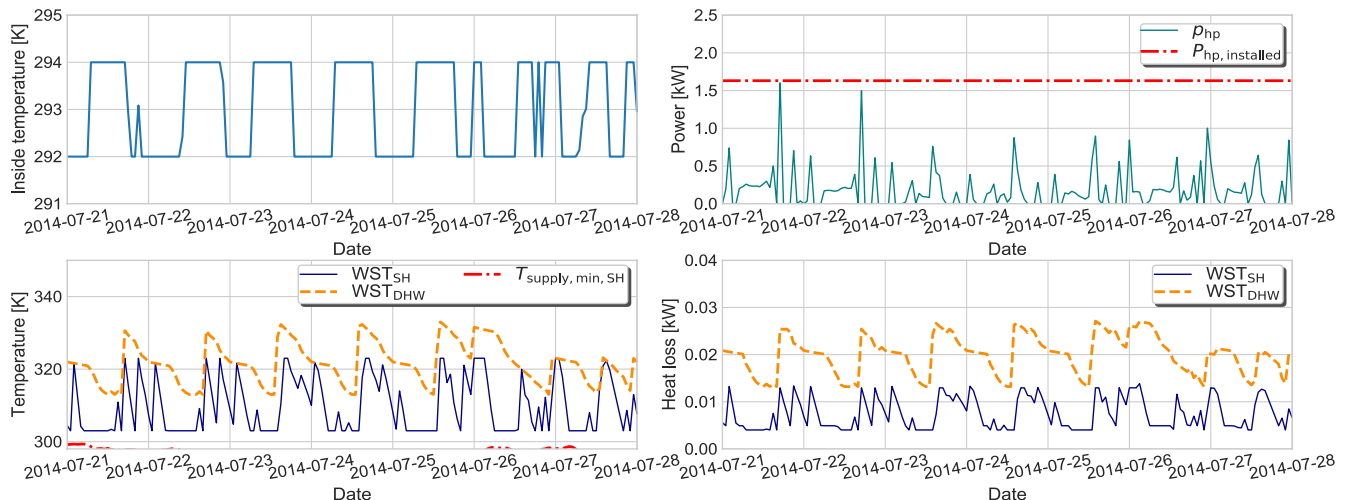

**Fig. 7.** Single household operation during a summer week for the ASHP and WST.

Table 4

Results on several environmental performance indicators, annual CO_2-emissions are average annual values. CO_2-avoided and CO_2-intensity are based on the system lifetime. These are all average annual values for a household in the community.

	Baseline	HES_{std}	HES_{opt}	CES_{opt}	Unit
Annual CO_2-emissions	3834[a]	298	334	334	[kg CO_2-eq./year]
CO_2-avoided	0	61964	62359	62821	[kg CO_2-eq./lifetime]
CO_2-intensity	–	0.080	0.078	0.076	[kg CO_2-eq./kW h]

[a] Emission factors baseline: 0.234 kg CO_2-eq./kW h heat for natural gas ("market for heat, central or small-scale, natural gas (CH)" [65]) and 0.083 kg CO_2-eq./kW h electricity, which is based on the mean of CO_2-emissions of the Swiss Times Energy system Model.
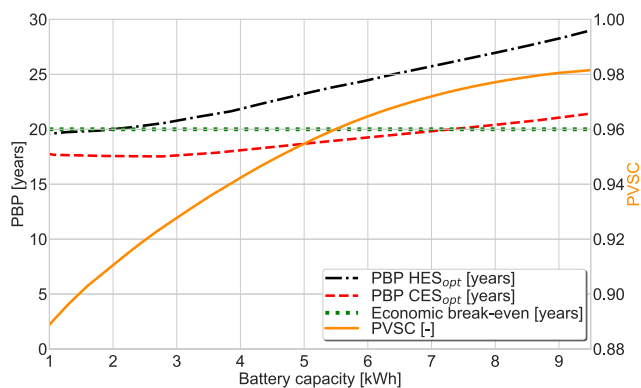
Fig. 8. Relation between PBP, battery capacity and PVSC of the optimally sized battery alternatives.
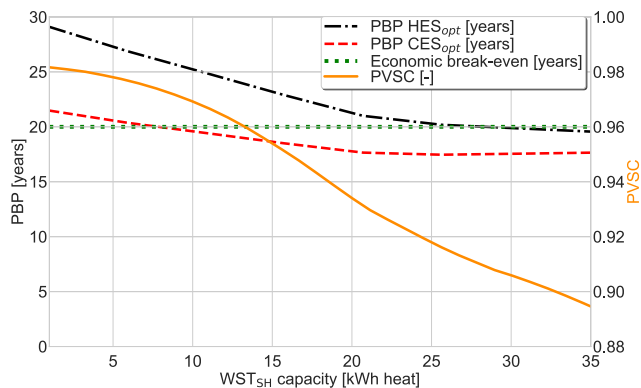
Fig. 9. Relation between PBP, WST_{SH} capacity and PVSC of the optimally sized battery alternatives.

This sensitivity analysis demonstrates that it could be economically beneficial to choose a larger sized WST_{SH}. Especially, a larger WST_{SH} capacity is preferred when the heat demand share (of the total energy) of the household is high. In this case, more energy can be stored as heat by a cheaper storage medium, such as a WST, while the PVSC remains high.

8. Discussion

8.1. Case study

The optimization model is tested on one Swiss case study only. To increase reliability of the results, the model requires testing under different conditions (e.g. different climate, size of communities and energy demands). For example, the performance of the system designs will be different in warmer climates since the CoP of the ASHP will increase [30] and the SH demand will be reduced. Furthermore, the system operation of this case study is based on CO_2-emissions from the Swiss electricity grid. However, grid CO_2-emissions in Switzerland are low in comparison with other countries.

In addition, this case study is based on Swiss policy, where no feed-in tariffs are provided for small PV installations (from 2 to 10 kW$_p$) [7]. The results will be different when feed-in tariffs are implemented. In this case, more profit can be made when electricity is injected into the grid when the feed-in tariff is high enough.

8.2. Model

We have developed an off-line optimization problem with perfect knowledge on load demand profiles, PV generation and using a similar charging pattern of BEVs for all households. In reality, demand loads and PV generation are volatile and have a stochastic nature [66]. Stochastic optimization algorithms and forecasting techniques can be used to accommodate the uncertainty in loads and PV generation profiles which could inevitably affect the results due to forecasting errors. Consequently, this means that the economic and environmental potential could be lower in the on-line optimization performed by the EMS. Therefore, we recommend to perform on-line optimization frameworks in future research in order to include the uncertainty of energy loads and PV generation. On the other hand, the implementation of on-line optimization frameworks, in combination with the inclusion of stochastic parameters, could increase the complexity and calculation time significantly.

A CoP prediction model is required as input for the optimization model. However, the accuracy of the CoP calculation can be improved by calculating the CoP per timestep based on additional parameters of the ASHP, such as the part load ratio [31]. On the other hand, these factors increase the calculation time and complexity of the model, since this could result in a non-linear optimization problem. Furthermore, the optimization model is designed at hourly resolution due to lack of data with a higher time resolution. The accurateness of the results can be improved by using a higher time resolution.

The focus of our work is on one system design (with a battery, ASHP and a combined WST). However, many different systems (e.g. district heating and geothermal heat) and storage designs (e.g. hydrogen storage and fuel cells) are possible hence different technologies can be combined [11,12].

For simplicity, the total storage capacity (for battery and WST together) size is set to store 90% of the daily grid injection of each household. However, the work of [16] emphasized that the implementation of this sizing methodology could result in significant differences in performance between households. This assumption is beneficial for some households, while others households show less beneficial economic performance. Therefore, the comparison between the optimally sized alternatives (HES_{opt} and CES_{opt}) with HES_{std} is not entirely fair. The difference between HES_{std} and the HES_{opt} and CES_{opt} alternatives could be bigger when the sizing methodology, for each household individually, is improved. For example, the sizing can be improved by including additional factors, such as the energy demand of a household.

8.3. Battery energy storage system

We assume that the battery capacity is stable during system lifetime. In reality, the capacity and performance of batteries degrade per charging/discharging cycle and by time (calendar losses) [23]. These factors are not included, but are of high importance since these can reduce the battery capacity and economic performance [67].

In addition, we only include CO_2-emissions as environmental indicator. However, due to the expected rise of the adoption of solar PV and battery, other environmental factors can be problematic [59]. For

instance, materials abundant in renewable energy technologies are finite hence energy systems need to be assessed on additional environmental indicators.

We do not consider the future development of battery costs although different research (e.g. [68]) demonstrates that battery costs will decrease into the coming years. This could result in a better economic and environmental performance of the proposed system designs. More specifically, [68] shows that battery costs for residential battery systems can be reduced to 400 euro/kW h in the year 2040. In this case, the HES$_{opt}$ shows a profitable system design with a PBP of 18.8 years. This emphasizes that the proposed system designs can have future potential hence future assessments are recommended.

Furthermore, we assume that the investment costs of the battery in CES are significantly lower compared to HES. However, the authors of [16] emphasize that the future reduction of battery costs for HES might be higher (compared to CES), due to the need for more complicated algorithms for communication systems in CES. Therefore, the future potential in CES could be less attractive than in HES.

8.4. Social factors

Social factors are not included in our work. However, these factors are essential to implement renewable energy technologies [69]. Furthermore, the benefits and drawbacks of the different storage scenarios (HES and CES) are not discussed. For example, CES offers additional benefits to end-user customers since the storage unit is not installed inside households. This avoids safety issues related to batteries, and this increases the comfort of residents. On the other hand, different research shows the complexity of CES [17], related to the distribution of shares of community components which are often based on complex algorithms.

8.5. Business models and other applications

We limit our assessment to the PVSC application and demand load shifting. Additional benefits and business models of HES and CES are not included. However, [13] demonstrate that additional benefits can be obtained from CES systems. For instance, CES can offer distributed applications such as peak shaving, voltage control and power to ancillary service markets.

Furthermore, we did not analyze the benefit of the aggregation of demand loads in the CES system. However, the controlling of CES is expected to be more convenient than the controlling of HES, since HES contains of more individual system components [8]. For example, a CES system would require only one measurement, communication system and EMS. Whereas the aggregation in HES, would require individual communication systems with every battery in each household.

9. Conclusions

Our work aimed to determine costs and CO_2-emissions of all-electric alternatives to substitute current fossil-fuel based residential energy supply. This paper started with a description of two system designs: HES and CES. For CES, this resulted in bigger sized system components in comparison with HES. Next, a multi-objective optimization model

Appendix A. Techno-economic parameters

Tables 5–9.

was developed to determine the optimal system operation based on costs and CO_2-emissions, while including promising technologies (e.g. batteries, WSTs and ASHPs) and load flexibility (BEVs and ASHPs). This paper included two HES alternatives (HES$_{std}$, HES$_{opt}$) and one CES alternative (CES$_{opt}$) to substitute the baseline scenario, where electricity was entirely absorbed from the electricity grid and heat demand was provided by natural gas. The HES$_{std}$ alternative contained of standardized batteries, while the battery of HES$_{opt}$ and CES$_{opt}$ were sized to reduce grid injection of self-produced PV electricity. These alternatives were tested on a community situated in Cernier (Switzerland).

The results demonstrate that the lowest operation costs (i.e. electricity bill) and CO_2-emissions are obtained from HES$_{std}$, followed by CES$_{opt}$ and HES$_{opt}$. However, the differences are small and HES$_{std}$ can hardly benefit from a larger sized battery. The results are fundamentally changed when the system lifetime is considered. In this way, CES$_{opt}$ performs best on both costs and CO_2-emissions, followed by HES$_{opt}$ and HES$_{std}$, respectively.

At the moment, none of the proposed alternatives is economically feasible due to high battery and ASHP costs. However, the economic performance of CES$_{opt}$ and HES$_{opt}$ can be improved when the battery storage size is reduced and the WST storage size is increased. This could result in a profitable system design for both CES$_{opt}$ and HES$_{opt}$. This demonstrates that a WST is a promising addition to batteries in the short-term. Especially, when battery costs and residential heat demand remain high.

We recommend to consider optimal sizing of the battery and WST based on households characteristics, such as energy demand and PV grid injection. With high heat demand, we argue to choose a larger WST to reduce costs. While with low heat demand and (future) low battery costs, a battery presents a storage medium with a higher storage quality. This work demonstrates that costs and CO_2-emissions can be significantly reduced due to economies of scale and household-specific sizing in a CES approach. Therefore, we recommend to adopt a CES approach for end-user customers and we argue to examine CES on other performance indicators (e.g. social and environmental).

Furthermore, it could be interesting to investigate potential benefits of CES and HES to other stakeholders. For example, distribution system operators and transmission system operators are of high importance to accelerate the implementation of alternative energy systems. The aggregation of demand profiles could help distribution system operators and transmission system operators with power applications, where additional economic and environmental value can be generated. To improve the economic feasibility of HES and CES, a future task is to compare the economic and environmental benefits of the proposed system designs for other stakeholders.

Acknowledgements

Table 5
Techno-economic parameters of battery.

Parameter	Value	Unit	Comment	Source
$\eta_{ch} = \eta_{dis}$	94.3	[%]		[23]
SoC_0	50	[%]		
SoC_{min}	3.5	[%]		[23]
SoC_{max}	96.5	[%]		[23]
$P^i_{grid,max}$	8	[kW]		
$P^i_{bat,max} : C^i_{bat}$	1:2	[kW:kW h]	Power: storage ratio (PVSC)	[23]
Lifetime (pack)	12	[Years]	NMC battery, Most likely value	[23,59]
Lifetime (BoS)	20	[Years]	NMC battery	[23]
Costs				
Battery pack cost	335	[euro/kW h]	NMC battery, Most likely value	[23]
BoS	2187	[euro/kW]	NMC battery, Most likely value	[23]
Maintenance	0	[euro/kW]	NMC battery, Most likely value	[23]
$CO_2 emissions$				
Production	108.3	[kg CO_2/kW h]	NMC battery	[23]
EMS & BMS	26.6	[kg CO_2/kW h]	General value for different batteries	[23]
PCS: home system (HES)	88.9	[kg CO_2-eq./kW]	Small battery (HES)	[23]
PCS: container system (CES)	28.2	[kg CO_2-eq./kW]	Large battery (CES)	[23]

Table 6
Techno-economic parameters of ASHP.

Parameter	Value	Unit	Comment	Source
$T^i_{building,min}$	292	[K]		
$T^i_{building,max}$	294	[K]		
$P^i_{ramprate,max}$	2	[kW]	Assumption	
Costs				
Installation	2000	[euro/unit]		[32]
Investment	1500	[euro/kW heat]		[32]
Maintenance	1.1	[% of investment/year]		[32]
Lifetime	20	[Years]		[32]
CO_2-*emissions*				
Production (HES & CES)	1.39E + 02	[kg CO_2-eq./kW heat]	"Heat pump production, brine-water, 10 kW (CH)" Extrapolated from 10 to 1 kW	[65]

Table 7
Techno-economic parameters of BEV.

Parameter	Parameter	Unit	Comment	Source
P^a_{min}	0	[kW]		
P^a_{max}	1.4	[kW]		[17]
Travelling distance	36.8	[km/day]		[62]
Fuel consumption	19.5	[kW h/100 km]		[63]

Table 8
Techno-economic parameters of PV panels.

Parameters	Value	Unit	Comment	Source
Rooftop area available	19.6	[m^2]	Approximated rooftop area	[53]
efficiency inverter	96	[%]	Nominal efficiency	[54]
Costs				
Module	898	[euro/kWp]	Maximum 2020 value, 6 kW, converted to euros	[46]
Labor	460	[euro/kWp]	Maximum 2020 value, 6 kW, converted to euros	[46]
Other cost	146	[euro/kWp]	Maximum 2020 value, 6 kW, converted to euros	[46]
Inverter	195	[euro/kWp]	Maximum 2020 value, 6 kW, converted to euros	[46]
BoS	209	[euro/kWp]	Maximum 2020 value, 6 kW, converted to euros	[46]
Maintenance	84	[euro/kWp/year]	Maximum 2020 value, 6 kW, converted to euros	[46]
Lifetime	30	[Years]		[46]
Remuneration PV	30	[%]	Of initial investment	[46]
CO$_2$-emissions				
Production	2368	[kg CO$_2$-eq./kWp]	"Photovoltaic slanted-roof installation, 3 kWp, multi-Si, panel, mounted, on roof (CH)"	[65]

Table 9
Techno-economic parameters of WST.

Parameters	Value	Unit	Comment	Source
U_{tank}	5.48E−01	[W m^{-2}K^{-1}]		[14]
c	1.16E−03	[kW h kg^{-1} K^{-1}]		
$T_{\text{SH,min}}^i$	303	[K]		[30]
$T_{\text{SH,max}}^i$	323	[K]		[30]
$T_{\text{DHW,min}}^i$	313	[K]		[30]
$T_{\text{DHW,max}}^i$	333	[K]		[30]
ρ_{water}	0.997	[kg/l]		
Height WST	1	[m]		
n_{persons}^i	2	[persons/hh]	Assumption	
Storage dimension	cylinder	[−]		
Costs				
Investment	120	[euro/kW h heat]	2016 value, 10 kW, ΔK of 20	[32]
Maintenance	0	[euro/kW h heat]	2016 value, 10 kW	[32]
Lifetime	20	[Years]	2016 value, 10 kW	[32]
CO$_2$-emissions				
Production (HES)	1.31E + 00	[kg CO$_2$-eq./l]	"Hot water tank production, 600 l (CH)"	[65]
Production (CES)	4.82E−01	[kg CO$_2$-eq./l]	"Heat storage production, 2000 l (CH)"	[65]

Appendix B. Inputs household operation
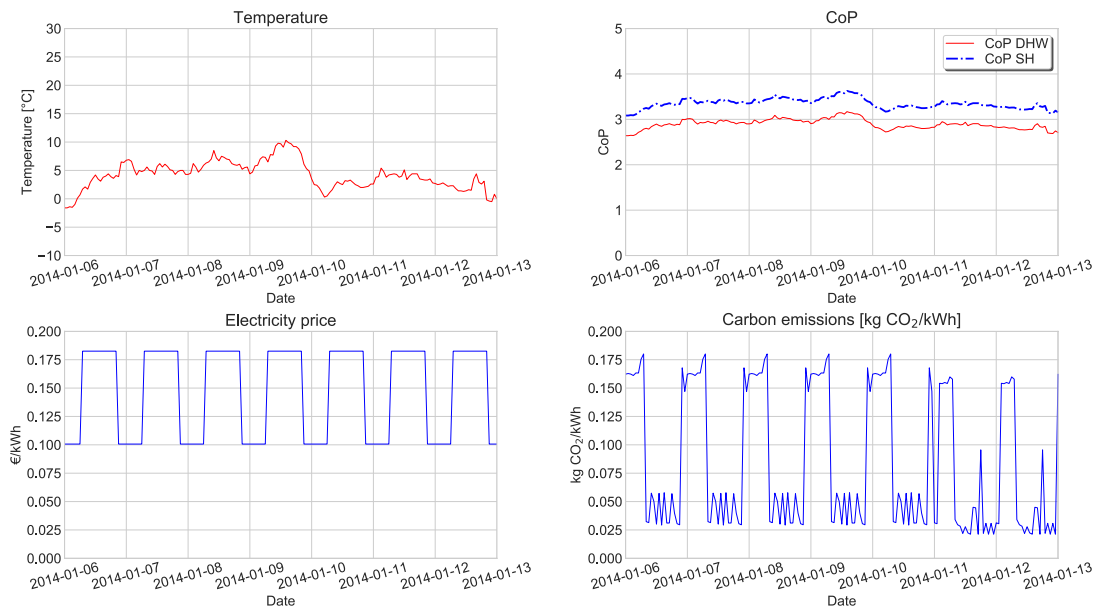
Figs. 10 and 11.

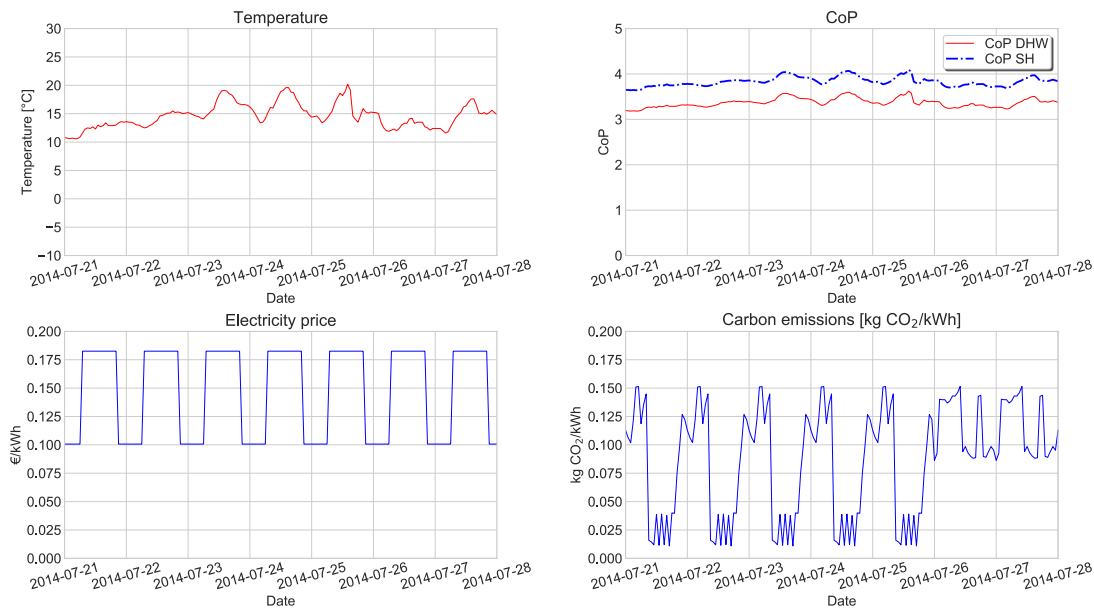**Fig. 10.** Inputs for single household operation during a winter week.

Fig. 11. Inputs for single household operation during a summer week.

References

[1] Gul MS, Patidar S. Understanding the energy consumption and occupancy of a multi-purpose academic building. Energy Build 2015;87:155–65. https://doi.org/10.1016/j.enbuild.2014.11.027.

[2] IEA. Transition to sustainable buildings, IEA. 2013. https://doi.org/10.1787/9789264202955-en < https://www.iea.org/publications/freepublications/publication/Building2013_free.pdf > .

[3] IRENA. Global Energy Transformation: A roadmap to 2050, Tech. rep., IRENA, Abu Dhabi; 2018. < http://www.irena.org/publications/2018/Apr/Global-Energy-Transition-A-Roadmap-to-2050 > .

[4] Ragwitz M, Winkler J, Klessmann C, Gephart M, Resch G. Recent developments of feed-in systems in the EU – a research paper for the International Feed-In Cooperation. Tech rep. Fraunhofer ISI; 2012.

[5] Couture T, Gagnon Y. An analysis of feed-in tariff remuneration models: implications for renewable energy investment. Energy Policy 2010;38(2):955–65. https://doi.org/10.1016/j.enpol.2009.10.047.

[6] IRENA. Adapting renewable energy policies to dynamic market conditions. Tech rep. May, IRENA; 2014. < http://www.irena.org/-/media/Files/IRENA/Agency/Publication/2014/policy_adaptation.pdf > .

[7] BFE. Wichtigste Neuerungen im Energierecht ab 2018; 2017. < http://www.bfe.admin.ch/energiestrategie2050/index.html?lang=de&dossier_id=06919 > .

[8] Parra D, Swierczynski M, Stroe DI, Norman SA, Abdon A, Worlitschek J, et al. An interdisciplinary review of energy storage for communities: challenges and perspectives. Renew Sust Energy Rev 2017;79:730–49. https://doi.org/10.1016/j.rser.2017.05.003.

[9] IEA. Technology roadmap solar photovoltaic energy. IEA; 2014. doi:https://doi.org/10.1007/SpringerReference_7300. < https://www.iea.org/publications/freepublications/publication/TechnologyRoadmapSolarPhotovoltaicEnergy_2014edition.pdf > .

[10] Matallanas E, Castillo-Cagigal M, Gutiérrez A, Monasterio-Huelin F, Caamaño-Martín E, Masa D, et al. Neural network controller for active demand-side management with PV energy in the residential sector. Appl Energy 2012;91(1):90–7. https://doi.org/10.1016/j.apenergy.2011.09.004.

[11] Alva G, Lin Y, Fang G. An overview of thermal energy storage systems. Energy 2018;144:341–78. https://doi.org/10.1016/j.energy.2017.12.037.

[12] Zakeri B, Syri S. Electrical energy storage systems: a comparative life cycle cost analysis. Renew Sust Energy Rev 2015;42:569–96. https://doi.org/10.1016/j.rser.2014.10.011.

[13] Arghandeh R, Woyak J, Onen A, Jung J, Broadwater RP. Economic optimal operation of community energy storage systems in competitive energy markets. Appl

Energy 2014;135:71–80. https://doi.org/10.1016/j.apenergy.2014.08.066.

[14] Parra D. Optimum community energy storage for end user applications. PhD Doctorate.

[15] Parra D, Norman SA, Walker GS, Gillott M. Optimum community energy storage system for demand load shifting. Appl Energy 2016;174:130–43. https://doi.org/10.1016/j.apenergy.2016.04.082.

[16] van der Stelt S, AlSkaif T, van Sark W. Techno-economic analysis of household and community energy storage for residential prosumers with smart appliances. Appl Energy 2018;209:266–76. https://doi.org/10.1016/j.apenergy.2017.10.096.

[17] AlSkaif T, Luna AC, Zapata MG, Guerrero JM, Bellalta B. Reputation-based joint scheduling of households appliances and storage in a microgrid with a shared battery. Energy Build 2017;138:228–39. https://doi.org/10.1016/j.enbuild.2016.12.050.

[18] Abdon A, Zhang X, Parra D, Patel MK, Bauer C, Worlitschek J. Techno-economic and environmental assessment of stationary electricity storage technologies for different time scales. Energy 2017;139:1173–87. https://doi.org/10.1016/j.energy.2017.07.097.

[19] Terlouw T, AlSkaif T, Bauer C, van Sark W. Multi-objective optimization of energy arbitrage in community energy storage systems using different battery technologies. Appl Energy 2019;239:356–72. https://doi.org/10.1016/j.apenergy.2019.01.227.

[20] van der Kam M, van Sark W. Smart charging of electric vehicles with photovoltaic power and vehicle-to-grid technology in a microgrid; a case study. Appl Energy 2015;152:20–30. https://doi.org/10.1016/j.apenergy.2015.04.092.

[21] Fischer D, Madani H. On heat pumps in smart grids: a review. Renew Sust Energy Rev 2017;70:342–57. https://doi.org/10.1016/j.rser.2016.11.182.

[22] Hirsch A, Parag Y, Guerrero J. Microgrids: a review of technologies, key drivers, and outstanding issues. Renew Sust Energy Rev 2018;90:402–11. https://doi.org/10.1016/j.rser.2018.03.040.

[23] Schmidt TS, Beuse M, Zhang X, Steffen B, Schneider SF, Pena-Bello A, et al. Additional emissions and cost from storing electricity in stationary battery systems. Environ Sci Technol 2019;53(7):3379–90. https://doi.org/10.1021/acs.est.8b05313.

[24] Sardi J, Mithulananthan N, Gallagher M, Hung DQ. Multiple community energy storage planning in distribution networks using a cost-benefit analysis. Appl Energy 2017;190:453–63. https://doi.org/10.1016/j.apenergy.2016.12.144.

[25] Gabrielli P, Gazzani M, Martelli E, Mazzotti M. Optimal design of multi-energy systems with seasonal storage. Appl Energy 2018;219:408–24. https://doi.org/10.1016/j.apenergy.2017.07.142.

[26] Parra D, Norman SA, Walker GS, Gillott M. Optimum community energy storage for renewable energy and demand load management. Appl Energy 2017;200:358–69. https://doi.org/10.1016/j.apenergy.2017.05.048.

[27] Wang H, Good N, Mancarella P. Economic analysis of multi-service provision from pv and battery based community energy systems; 2017. p. 1–6. doi:https://doi.org/10.1109/ISGT-Asia.2017.8378390.

[28] Baldick R. Applied optimization: formulation and algorithms for engineering systems vol. 9780521855. University of Texas; 2006. https://doi.org/10.1017/CBO9780511610868.

[29] Mesarić P, Krajcar S. Home demand side management integrated with electric vehicles and renewable energy sources. Energy Build 2015;108:1–9. https://doi.org/10.1016/j.enbuild.2015.09.001.

[30] Staffell I, Brett D, Brandon N, Hawkes A. A review of domestic heat pumps. Energy Environ Sci 2012;5(11):9291. https://doi.org/10.1039/c2ee22653g.

[31] Fischer D, Wolf T, Wapler J, Hollinger R, Madani H. Model-based flexibility assessment of a residential heat pump pool. Energy 2017;118:853–64. https://doi.org/10.1016/j.energy.2016.10.111.

[32] Fischer D, Lindberg KB, Madani H, Wittwer C. Impact of PV and variable prices on optimal system sizing for heat pumps and thermal storage. Energy Build 2016;128:723–33. https://doi.org/10.1016/J.ENBUILD.2016.07.008.

[33] Saraf N. Predictive control for residential capacity controlled heat pumps in a smart grid scenario N. Saraf. Master thesis.

[34] Department of Energy & Climate Change. Potential cost reductions for air source heat pumps. Tech rep. Department of Energy & Climate Change; 2016. < https://assets.publishing.service.gov.uk/government/uploads/system/uploads/attachment_data/file/498962/150113_Delta-ee_Final_ASHP_report_DECC.pdf > .

[35] Gurobi. Gurobi optimization – the state-of-the-art mathematical programming solver; 2018. < http://www.gurobi.com/.

[36] Hamdy M, Hasan A, Siren K. Applying a multi-objective optimization approach for design of low-emission cost-effective dwellings. Build Environ 2011;46(1):109–23. https://doi.org/10.1016/j.buildenv.2010.07.006.

[37] Fesanghary M, Asadi S, Geem ZW. Design of low-emission and energy-efficient residential buildings using a multi-objective optimization algorithm. Build Environ 2012;49(1):245–50. https://doi.org/10.1016/j.buildenv.2011.09.030.

[38] Protopapadaki C, Saelens D. Heat pump and pv impact on residential low-voltage distribution grids as a function of building and district properties. Appl Energy 2017;192:268–81. https://doi.org/10.1016/j.apenergy.2016.11.103.

[39] Hellweg S, Milà i Canals L. Emerging approaches, challenges and opportunities in life cycle assessment. Science (New York, NY) 2014;344(6188):1109–13. https://doi.org/10.1126/science.1248361.

[40] ISO. ISO 14040: life cycle assessment, principles and framework, environmental

[41] ISO. ISO 14044: life cycle assessment – requirements and guidelines; 2006. doi:https://doi.org/10.1136/bmj.332.7550.1107.

[42] Wernet G, Bauer C, Steubing B, Reinhard J, Moreno-Ruiz E, Weidema B. The ecoinvent database version 3 (part I): overview and methodology. Int J Life Cycle Assess 2016;21(9):1218–30. https://doi.org/10.1007/s11367-016-1087-8.

[43] IPCC. Fifth assessment report – climate change. 2013.

[44] Frischknecht R, Fantke P, Tschümperlin L, Niero M, Antón A, Bare J, et al. Global guidance on environmental life cycle impact assessment indicators: progress and case study. Int J Life Cycle Assess 2016;21(3):429–42. https://doi.org/10.1007/s11367-015-1025-1.

[45] Baumann M, Peters DJ, Weil DiM, Grunwald PDA. CO2 footprint and life-cycle costs of electrochemical energy storage for stationary grid applications. Energy Technol 2017;5:1071–83. https://doi.org/10.1002/ente.201600622.

[46] Bauer C, Hirschberg S, Bäuerle Y, Biollaz S, Calbry-Muzyka BC, Heck T, et al. Potentials, costs and environmental assessment of electricity generation technologies. Tech rep. PSI, WSL, ETHZ, EPFL. Paul Scherrer Institut, Villigen PSI, Switzerland; 2017.

[47] Weber S, Puddu S, Pacheco D. Move it! How an electric contest motivates households to shift their load profile. Energy Econ 2017;68:255–70. https://doi.org/10.1016/j.eneco.2017.10.010.

[48] MeteoSwiss. MeteoSwiss IDAWEB; 2018.

[49] Wang D, Landolt J, Mavromatidis G, Orehounig K, Carmeliet J. CESAR: a bottom-up building stock modelling tool for Switzerland to address sustainable energy transformation strategies. Energy Build 2018;169:9–26. https://doi.org/10.1016/j.enbuild.2018.03.020.

[50] Fischer D, Wolf T, Scherer J, Wille-Haussmann B. A stochastic bottom-up model for space heating and domestic hot water load profiles for German households. Energy Build 2016;124:120–8. https://doi.org/10.1016/j.enbuild.2016.04.069.

[51] Kannan R, Turton H. Long term climate change mitigation goals under the nuclear phase out policy: the Swiss energy system transition. Energy Econ 2016;55:211–22. https://doi.org/10.1016/j.eneco.2016.02.003.

[52] Andrews RW, Stein JS, Hansen C, Riley D. Introduction to the open source PV LIB for python Photovoltaic system modelling package. In: 2014 IEEE 40th photovoltaic specialist conference, PVSC 2014; 2014. p. 170–4. doi:https://doi.org/10.1109/PVSC.2014.6925501.

[53] Margelou S. Assessment of long term solar PV diffusion in Switzerland. Master thesis; 2015. p. 75.

[54] Dobos AP. PVWatts version 5 manual. Tech rep. NREL; 2014.

[55] Boogen N, Datta S, Filippini M. Demand-side management by electric utilities in Switzerland: analyzing its impact on residential electricity demand. Tech rep. May, SCCER CREST; 2016. < https://www.sccer-crest.ch/fileadmin/FILES/Datenbank_Personen_Projekte_Publikationen/Publications/Working_Papers/Work_Package_2/Boogen_Datta_Filippini_2016_Demand-side_management.pdf > .

[56] Groupe-e. Tarif unique Tarif double/Doppeltarif ehemals Easy; 2018.

[57] Kannan Ramachandran, Turton H. Switzerland energy transition scenarios development and application of the swiss times energy system model (stem). Tech rep. 14, PSI; 2014.

[58] Swissgrid. Grid data; 2018. < https://www.swissgrid.ch/en/home/operation/grid-data.html > .

[59] Terlouw T, Zhang X, Bauer C, Alskaif T. Towards the determination of metal criticality in home-based battery systems using a Life Cycle Assessment approach. J Clean Prod 2019;221:667–77. https://doi.org/10.1016/j.jclepro.2019.02.250.

[60] Nitta N, Wu F, Lee JT, Yushin G. Li-ion battery materials: present and future. Mater Today 2015;18(5):252–64. https://doi.org/10.1016/j.mattod.2014.10.040.

[61] Tesla. Powerwall; 2018. > < https://www.tesla.com/sites/default/files/pdfs/powerwall/Powerwall%202_AC_Datasheet_en_northamerica.pdf > .

[62] BFS. Bevölkerung verbringt täglich eineinhalb Stunden im Verkehr. Tech rep. BFS; 2017.

[63] Cox B. Mobility and the energy transition: a life cycle assessment of swiss passenger transport technologies including developments until 2050. Phd thesis, ETHZ; 2018. < https://www.research-collection.ethz.ch/handle/20.500.11850/276229 > .

[64] Schweizerische Eidgenossenschaft. Eidg. Volkswirtschaftsdepartement EVD – Preisüberwachung; 2018. < http://gaspreise.preisueberwacher.ch/web/index.asp?z=5&codekategorie=TypII > .

[65] Ecoinvent, ecoinvent 3.4; 2018. < https://www.ecoinvent.org/database/ecoinvent-34/ecoinvent-34.html > .

[66] Antonanzas J, Osorio N, Escobar R, Urraca R, de Pison FM, Antonanzas-Torres F. Review of photovoltaic power forecasting. Solar Energy 2016;136:78–111. https://doi.org/10.1016/j.solener.2016.06.069.

[67] Xu B, Zhao J, Zheng T, Litvinov E, Kirschen DS. Factoring the cycle aging cost of batteries participating in electricity markets. IEEE Trans Power Syst 2018;33(2):2248–59. https://doi.org/10.1109/TPWRS.2017.2733339.

[68] Schmidt O, Hawkes A, Gambhir A, Staffell I. The future cost of electrical energy storage based on experience rates. Nat Energy 2017;2:1–8. https://doi.org/10.1038/nenergy.2017.110.

[69] AlSkaif T, Lampropoulos I, van den Broek M, van Sark W. Gamification-based framework for engagement of residential customers in energy applications. Energy Res Soc Sci 2018;44:187–95. https://doi.org/10.1016/j.erss.2018.04.043.